Conventional and advanced exergy-exergoeconomic-exergoenvironmental analyses of an organic Rankine cycle integrated with solar and biomass energy sources

Xinrui Qi
School of Engineering
Ocean University of China
Qingdao 266100, China
Email: qxr@stu.ouc.edu.cn

Chunsheng Yang
Aerospace Research Centre
National Research Council Canada
Ottawa, K1A 0R6, Canada
Email: chunsheng.yang@nrc-cnrc.gc.ca

Mingyang Huang, Zhenjun Ma
Sustainable Buildings Research Centre
University of Wollongong
Wollongong, NSW2522, Australia
Email: mh784@uowmail.edu.au & zhenjun@uow.edu.au

Anna Hnydiuk-Stefan
Faculty of Production Engineering and Logistics
Opole University of Technology
Opole 45-758, Poland
Email: a.hnydiuk-stefan@po.edu.pl

Ke Feng
Department of Industrial Systems Engineering and Management
National University of Singapore
117576, Singapore
Corresponding authors.
Email: ke.feng@outlook.com.au

Patrick Siarry
Laboratory of Images, Signals and Intelligent Systems
University Paris-Est Créteil Val de Marne
Creteil 94010, France
Email: siarry@u-pec.fr

Grzegorz Królczyk & Z Li
Faculty of Mechanical Engineering
Opole University of Technology
Opole 45-758, Poland
Email: g.krolczyk@po.opole.pl; z.li@po.edu.pl

Corresponding Author: z.li@po.edu.pl

Abstract

Considering the huge consumption of traditional energy and the rising demand for electricity, the development of renewable energy is very necessary. In this paper, an energy system integrating biomass energy, solar and two-stage organic Rankine cycle (ORC) is proposed, which uses the stable energy output of biomass energy to compensate for the volatility of solar modules. The proposed system comprises a biomass boiler, photovoltaic thermal panels (PV/T), evaporators, condensers, working medium pumps, turbines, a preheater and an air preheater. In addition, conventional and advanced exergy, exergoeconomic and exergoenvironmental (3E) analyses are carried out. Conventional 3E analyses reveal two components that require priority improvement. They are respectively evaporator 1 with the largest exergy destruction (708.2kW) and exergy destruction environmental impact rate (775.3 mPt/h) and evaporator 2 with the largest exergy destruction cost rate (19.15$/h). The results of advanced 3E analyses show that the largest avoidable endogenous exergy destruction is condenser 1 (136.6kW), the largest avoidable endogenous exergy destruction cost rate is condenser 2 (3.377$/h), and the largest avoidable endogenous exergy destruction environmental impact rate is condenser 1 (196.1mPt/h). These mean that these components have great potential for improvement in reducing exergy destruction, saving cost and protecting the environment. In addition, the avoidable endogenous exergy destruction/cost/environmental impact rate of evaporator 2 are negative, so evaporator 2 is not suitable as a priority component for improvement, which is contrary to the conclusions of conventional 3E analyses. It is found that conventional 3E analyses can only point out the biggest exergy destruction point, but cannot indicate whether the components with the greatest exergy destruction have the greatest potential for improvement. However, advanced 3E analyses can show the improvement

potential of each component by improving its own performance and the external conditions. Therefore, it is necessary to conduct advanced 3E analyses.

Keywords: Exergoenvironmental analysis, Exergoeconomic analysis, Advanced exergy, Two-state ORC.

1 Introduction

The huge consumption of fossil fuels and the environmental impact of greenhouse gas emissions have become hot topics at present. Humanity is trying to find environmentally friendly renewable energy sources alternative to traditional energy sources [1,2]. Due to the decreasing cost of solar power generation technology and biomass energy has the advantages of direct storage, transportation and widespread existence [3], so the two have great potential in the future development of renewable energy. However, solar energy is greatly affected by climate change, and the solar irradiance varies from region to region. Therefore, the reliability of solar energy is lower [4]. Biomass energy, on the other hand, is a renewable energy source that can be stored and transported directly. It is also another form of solar energy and can exist in solid, liquid or gaseous form. In addition, the carbon dioxide emitted during the biomass combustion process and the carbon dioxide absorbed during the biomass growth process offset each other to become a pollution-free renewable energy [3]. Combining the characteristics of the two energy sources, the comprehensive application of biomass energy and solar energy can effectively make up for the unstable output of solar energy caused by weather.

The electrical efficiency of solar photovoltaic panels is inversely correlated with the temperature of photovoltaic panels. Photovoltaic thermal panels (PV/T) effectively improve the power generation efficiency of photovoltaic panels by absorbing the heat of photovoltaic panels and then output low-grade thermal energy [5]. In addition, biomass-fired is an effective way to use biomass on a large scale [6,7]. The energy density of biomass energy is low, so the low-grade heat generated by the PV/T and biomass boilers can be recovered using the Organic Rankine Cycle (ORC). The Organic Rankine cycle is a good way to convert low-grade thermal energy into high-grade electricity. It is a feasible method for medium and low temperature heat source recovery. This cycle uses low boiling point organic fluids as the circulating working medium, compared to the Rankine cycle using water as the circulating working medium. Therefore, the ORC can recover heat sources with a temperature of 65-400°C [8]. In 2022, Atiz et al. [9] established the PV/T and ORC coupling model suitable for family load, and achieved cogeneration through the full use of heat sources. In the same year, Ding et al. [10] compared the economics of biomass gasification and biomass-fired for heating, and the results showed

that the total cost of biomass gasification technology was about 1.63 times that of biomass-fired, which confirmed the feasibility of coupling biomass-fired and the ORC.

In order to improve comprehensive performances of the ORC, many researchers have improved the ORC based on its working principle. They designed the recuperative organic Rankine cycle [11,12], the pumped recuperative organic Rankine cycle[13], the reheating-recuperation-internal recuperation organic Rankine cycle [14] and the dual organic Rankine cycle [15]. Zeng et al. [15] compares the three structures of the ORC, tandem ORC and double ORC based on cold condition, conventional condition and tropical condition, and the results show that the thermodynamic and economic performance of double ORC are the best under cold and conventional conditions. In tropical environments, tandem ORC have the best thermodynamic and economic performance. In summary, the improved tandem ORC and dual ORC are superior to the basic ORC in terms of thermodynamic performance and cost. Li et al. [16] designed an energy system integrated with geothermal energy, proton exchange membrane fuel cells and two-stage organic Rankine flash cycles. He cleverly used different heat source temperatures of geothermal energy and proton exchange membrane fuel cells, increasing the exergy efficiency of the system and greatly improving the net output power of the system. Therefore, the two-stage ORC cycle can be designed for two heat sources of biomass and solar output. This helps to make use of the temperature cascade and obtain better energy output.

Most current assessments of hybrid energy systems include conventional exergy analysis and exergoeconomic analysis [17–19], and a few studies include the exergoenvironmental analysis proposed by Meyer in 2009 [20]. These conventional exergy, exergoeconomic and exergoenvironmental (3E) analyses can determine the improvement potential of each component in the energy system. These methods divide the output of components into exergy destruction and useful energy, and calculate the economic and environmental impact caused by exergy destruction and useful energy. So as to optimize the energy system in a targeted manner. In 2023, Wang et al. [21] performed a conventional 3E analyses of an energy system integrating a biomass gasifier and solid oxide fuel cells. And they used the multi-objective particle swarm optimization algorithm to optimize three different kinds of double objectives. In 2023, Ali et al. [22] performed energy and exergy analyses on the combined cold, heat and electricity generation system integrated with the improved Kalina cycle and the supercritical CO_2 power cycle. They evaluated the system by energy efficiency and exergy efficiency. Khoshgoftar Manesh et al. [23] designed a polygeneration system powered by solar energy and natural gas. The energy, exergy, exergoeconomic and exergoenvironmental of the system were analyzed. Finally, multi-objective optimization method is used to optimize the integrated system.

However, the conventional 3E analyses still have some limitations. They only indicate in general terms the amount of energy lost during the operation of the components, and do not specify whether and how much energy loss can be reduced. Therefore, many researchers [24–26] have improved the conventional 3E analyses and proposed advanced exergy, advanced exergoeconomic and advanced exergoenvironmental analyses. Advanced 3E analyses separate exergy destruction, exergy destruction cost, and exergy destruction environmental impact in terms of endogenous/exogenous and avoidable/unavoidable, which helps to determine the ability of components to improve by optimizing their own efficiency and technical conditions.

In 2019, Moharramian et al. [27] conducted conventional and advanced exergy and exergoeconomic analyses of an energy system integrating biomass and photovoltaic hydrogen production, and discussed module parameters setting with exergy efficiency and exergoeconomic factor as evaluation indicators. In addition, the conclusions reached by conventional exergy and exergoeconomic analyses are not consistent with those reached by advanced exergy and exergoeconomic analyses. This suggests that conventional exergy analysis can point to the component that is most exergy destruction, but not the boostable potential of that component. In 2020, Oyekale et al. [28,29] conducted conventional and advanced exergy and exergoeconomic analyses of a cogeneration system integrated with solar, biomass, and an organic Rankine cycle. Two improvement methods for the exergoeconomic analysis are described, which provides a reference for system improvement. In 2020, Khoshgoftar Manesh et al. [30] evaluated the combined biomass gasification cycle using conventional and advanced 3E analyses, and explored the improvement potential of each component in the cycle. In 2021, Al-Sayyab et al. [31] evaluated a PV/T-driven ejector heat pump system using conventional and advanced exergy and exergoeconomic analyses. The results show that the improvement opinions given by conventional exergy analysis and advanced exergy analysis are similar. The results of Moharramian and Al-Sayyab suggest that conventional exergy analysis and advanced exergy analysis may have different results for different energy systems. In 2021, Wang et al. [32] used the organic Rankine cycle as an example to introduce in detail the process of advanced exergy analysis using thermodynamic cycle method. The gap between conventional exergy analysis and advanced exergy analysis was compared. He said advanced exergy analysis pinpoints the components with the greatest potential for improvement. Hu et al. [33] conducted conventional exergy analysis and advanced exergy analysis of the cascade high-temperature heat pump system based on experimental data, and determined the priority of system component improvement. In 2022, Dilek Nur et al. [34] analyzed a power generation system powered by the LNG using conventional and advanced

exergy and exergoeconomic analyses. They explored the components of the proposed system with the greatest potential for improvement. In 2022, Gürbüz et al. [35] conducted an exergoenvironmental analysis of an energy system coupled with geothermal energy and two-stage ORC. He divided environmental impacts into endogenous/exogenous and avoidable/unavoidable parts, and obtained information on the interactions between components and improvement potential from the perspective of environmental impact. In 2023, Zahra et al. [36] designed a triple generation power system powered by the geothermal energy, and they performed conventional and advanced exergy analyses on the system. Eventually they get a priority for component improvement. In 2023, Li et al. [37] proposed the organic Rankine flash cycle drived by geothermal energy, and they used conventional and advanced exergy and exergoeconomic analyses. The potential for improvement of the individual components of the system is obtained. In the same year, Tian et al. [38] performed conventional and advanced exergy analyses of the organic Rankine cycle for low temperature cold energy recovery. The results showed that the avoidable endogenous exergy destruction of the expander has the highest proportion of the total exergy destruction, so it has the best potential for improvement.

It is not difficult to see that conventional and advanced 3E analyses have quite good results for the optimization of renewable energy systems. However, there are currently little literatures on both conventional and advanced 3E analyses of energy systems. Many studies analyze only one or two of the conventional and advanced exergy, exergoeconomic, and exergoenvironmental [28,31,39]. As people pay more attention to the environment, environmental impact has become as much a part of the energy system design and optimization process as cost. In addition, conventional and advanced 3E analyses can determine the exergy destruction that can be reduced for each component of the energy system, and how to reduce the exergy destruction. These provide a good reference for the comprehensive optimization of energy system. Therefore, comprehensive conventional and advanced 3E analyses of the energy system are essential. The main work and novelty of this paper are summarized as follows:

- Designing a multi-energy complementary energy system of biomass energy and solar energy. It used two-stage organic Rankine cycle as waste heat recovery device for biomass boiler and the PV/T.
- Performing conventional 3E analyses of the energy system, especially exergoenvironmental analysis that is less frequently performed.
- Conducting advanced 3E analyses of the energy system to provide detailed advices for the proposed energy system.

2 System description

Figure 1 shows a schematic diagram of the proposed system. This system mainly consists of two parts. They are the organic Rankine cycle driven by boiler pressurized hot water and the organic Rankine cycle driven by the PV/T output hot water.

Biomass fuel and air preheated by an air preheater are fully burned in a biomass boiler and the heat is transferred to water to produce pressurized hot water. Pressurized hot water enters evaporator 1 and is then exchanged with the organic working medium R245fa in the ORC 1. After heat exchange, the pressurized hot water returns to the biomass boiler for further heating. These form a biomass boiler pressurized hot water cycle. The R245fa at the outlet of evaporator 1 is first pressurized by pump 1 and then absorbs heat in evaporator 1, so it becomes an organic fluid with high temperature and high pressure. This fluid enters the turbine to expand rapidly and then push the turbine to do work to generate electricity. After the work, the fluid still has residual heat, so it is designed to enter the preheater to preheat the high-pressure medium of the ORC 2, and reduce its own temperature to reduce the cooling water flow of condenser 1. Condenser 1 condenses the working fluid at the outlet of the preheater into a liquid and sends it to pump 1 for pressurization. The pressurized organic working fluid then enters evaporator 1 for evaporation. These create the ORC 1 cycle. The ORC 2 works similarly to the ORC 1, except that the heat source for evaporator 2 comes from the PV/T output hot water. The PV/T is a solar system for cogeneration. Cold fluid enters the PV/T module to take away the heat of the photovoltaic panels. This not only results in thermal fluids, but also improves the efficiency of photovoltaic cells. However, the PV/T operation is greatly affected by weather. In order to make the ORC 2 operation more stable, the design feeds a high-pressure organic working fluid that has been pressurized by pump 2 and preheated by preheater into the evaporator 2. The power generated by turbine 1, turbine 2 and the PV/T components is the main output of this system.

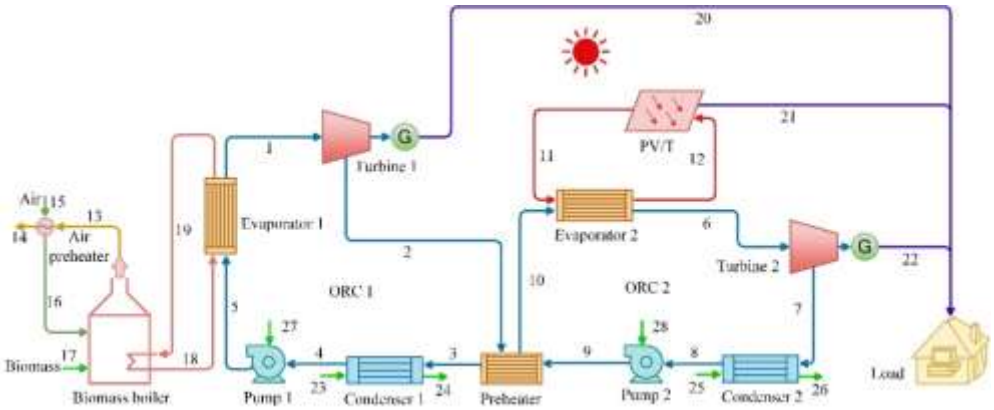

Figure 1 Schematic diagram of the proposed system.

3 Mathematical model

In this section, mathematical models related to energy, conventional exergy, conventional exergoeconomic, conventional exergoenvironmental, advanced exergy, advanced exergoeconomic and advanced exergyoenvironmental are established. Engineering Equation Solver and TRNSYS were used for simulation and calculation. To simplify the model, the following assumptions are made [40,41]:

(1) The system operation is steady-state;

(2) Ignoring the power consumption of the cooling water pump;

(3) Ignoring heat loss and pressure drop in components and pipings;

(4) The ambient temperature is 293.15K, and the ambient pressure is 101.325kPa;

(5) The isentropic efficiency of turbine and working medium pump is 0.85.

3.1 Energy analysis

Biomass-fired is the process of combustion reaction of biomass fuel in the burner, where the fuel used in the biomass burner is biomass pellet fuel. Its element analysis is shown in Table 1. The thermal efficiency of biomass pressurized hot water boiler is 0.9 [42] and the given heat load is 650kW. The biomass boiler heat balance calculation [43] is as follows:

$$\dot{Q}_{bio} = \dot{m}_{bio} \cdot LHV_{bio} \tag{1}$$

$$\dot{Q}_{in} = \dot{Q}_{bio} \cdot \eta_{bio} \tag{2}$$

where Q_{bio} is the given heat load of the biomass pressurized hot water boiler. $\dot{m}_{bf}$ is the mass flow rate of biomass pellet fuel. LHV_{bf} is the low heat value of biomass pellet fuel, and $LHV_{bf} = 17200kJ/kg$ [43]. Q_{in} is the heat of biomass boiler to pressurized hot water. η_{bio} is the thermal efficiency of biomass boiler.

Table 1 Elemental analysis of biomass pellet fuels.

Type	Value
C/%	48.01
H/%	6.39
O/%	33.83
N/%	0.47
S/%	0.13
Ash element/%	2.42

Moisture/%	8.7
Volatile/%	80.69

The amount of air required for combustion of the biomass boiler and the amount of flue gas emitted are calculated according to the data in Table 1 [43].

$$\dot{V}_{the,air} = 0.0899 \cdot (C + 0.375S) + 0.265H - 0.0333O \tag{3}$$

$$\dot{V}_{the,CO_2} = 1.866C \tag{4}$$

$$\dot{V}_{the,SO_2} = 0.67S \tag{5}$$

$$\dot{V}_{the,N_2} = 0.79\dot{V}_{the,air} + 0.8N \tag{6}$$

$$\dot{V}_{the,H_2O} = 0.111H + 0.0124M \tag{7}$$

$$\dot{V}_{the,fg} = \dot{V}_{the,CO_2} + \dot{V}_{the,SO_2} + \dot{V}_{the,N_2} + \dot{V}_{the,H_2O} \tag{8}$$

$$\dot{V}_{act,fg} = \dot{V}_{the,fg} + (\alpha - 1) \cdot \dot{V}_{the,air} + 0.016 \cdot (\alpha - 1) \cdot \dot{V}_{the,air} \tag{9}$$

$$\dot{m}_{air} = \alpha \cdot \dot{V}_{the,air} \cdot \rho_{air} \cdot \dot{m}_{bf} \tag{10}$$

$$\dot{m}_{CO_2} = \dot{V}_{the,CO_2} \cdot \rho_{CO_2} \cdot \dot{m}_{bf} \tag{11}$$

where $\dot{V}$ represents the amount of air entering the boiler and the amount of individual gases emitted by the boiler, $\dot{m}$ represents the mass flow, α is the excess air coefficient, and $\alpha = 1.6$ [44]. ρ represents density, and $\rho_{air} = 1.2048 kg/m^3, \rho_{CO_2} = 1.2283 kg/m^3$ [42]. The subscript the represents the theoretical value, act represents the actual value, and fg represents the flue gas emitted from the boiler.

The heat source of the air preheater is the high-temperature flue gas emitted from the biomass boiler. The outlet temperature of the flue gas is 439.65K [45]. The equation for the energy balance of an air preheater is as follows:

$$\dot{m}_{air} \cdot c_{air} \cdot (T_{16} - T_{15}) = \dot{m}_{fg} \cdot c_{fg} \cdot (T_{13} - T_{14}) \tag{12}$$

where c represents the specific heat capacity, T represents the temperature, and the subscripts of the number are derived from Figure 1.

The PV/T is a solar cogeneration system. It is an excellent choice for small household energy systems. Adding thermal conduction channels on the back of the PV/T and then entering cold fluid, which can not only reduce the temperature of photovoltaic panels to improve the efficiency of photovoltaic panels, but also absorb heat into low-grade heat energy. The total

amount of radiation and electricity production by photovoltaic panels are as follows [46–48]:

$$\dot{P}_{sun,PV/T} = G \cdot A_{PV/T} \cdot \tau_g \cdot \alpha_{cell} \tag{13}$$

$$\dot{W}_{PVT} = \alpha_{cell} \cdot \eta_{cell} \cdot \tau_g \cdot G \cdot A_{PV/T} \tag{14}$$

$$\eta_{cell} = \eta_{ref} \cdot (1 - \beta \cdot (T_{cell} - T_{ref})) \tag{15}$$

where G is the instantaneous irradiation intensity per unit area. $A_{PV/T}$ is the overall surface area of the PV/T, and $A_{PV/T}$=1000m^2. α_{cell} is the absorption rate of the PV/T, and α_{cell}=0.93 [9]. η_{pf} is the packing factor, and $\eta_{pf} = 0.8$. η_{ref} is the cell efficiency at T_{ref} temperature. T_{ref} is the reference temperature of the cell efficiency, and $T_{ref} = 298K$. τ_g is the cover transmittance of the PV/T glass, and $\tau_g = 0.83$ [49]. β is the temperature coefficient of solar cell efficiency, and β=0.005 [50]. T_{cell} is the photovoltaic cell temperature.

The organic Rankine cycle is an important part of the proposed system. The energy analysis of the components in the ORC 1 and the ORC 2 is shown in Table 2.

Table 2 Energy analysis equation for organic Rankine cycles.

Component	Energy balance equation	Notes
Condenser 1	$\dot{m}_{wf1} \cdot (h_3 - h_4) = \dot{m}_{cw1} \cdot c_{cw1} \cdot (T_{24} - T_{23})$	The h is the specific enthalpy, and the subscript $cw1$ represents the cooling water of condenser 1;
Condenser 2	$\dot{m}_{wf2} \cdot (h_7 - h_8) = \dot{m}_{cw2} \cdot c_{cw2} \cdot (T_{26} - T_{25})$	The subscript $cw2$ represents the cooling water of condenser 2;
Evaporator 1	$\dot{m}_{wf1} \cdot (h_1 - h_5) = \dot{m}_{bhw} \cdot c_{bhw} \cdot (T_{18} - T_{19})$	The subscript bhw represents boiler pressurized hot water;
Evaporator 2	$\dot{m}_{wf2} \cdot (h_6 - h_{10}) = \dot{m}_{PV/Thw} \cdot c_{PV/Thw} \cdot (T_{11} - T_{12})$	The subscript PV/Thw represents the PV/T output hot water;
Preheater	$\dot{m}_{wf1} \cdot (h_2 - h_3) = \dot{m}_{wf2} \cdot (T_{10} - T_9)$	The subscripts $wf1$ and $wf2$ represent the working fluids of the ORC 1 and ORC 2;
Pump 1	$\dot{W}_{pump1} = \dot{m}_{wf1} \cdot (h_5 - h_4)$	$\dot{W}_{pump1}$ represents the work consumed by pump 1;

Pump 2	$\dot{W}_{pump2} = \dot{m}_{wf2} \cdot (h_9 - h_8)$	$\dot{W}_{pump2}$ represents the work consumed by pump 2;
Turbine 1	$\dot{W}_{tur1} = \dot{m}_{wf1} \cdot (h_1 - h_2)$	$\dot{W}_{tur1}$ represents the work output of turbine 1;
Turbine 2	$\dot{W}_{tur2} = \dot{m}_{wf2} \cdot (h_6 - h_7)$	$\dot{W}_{tur2}$ represents the work output of turbine 2.

3.2 Conventional 3E analyses

Exergy refers to the part of energy that is available. The available energy in energy is only part of the energy, and the other part of the energy is often lost in the form of exergy destruction. The purpose of exergy analysis of the system is to calculate the exergy destruction of each component. Exergy analysis is also a powerful way to identify the energy quality of each component. It can help find the maximum point of exergy destruction in energy systems and provide reference for system performance optimization [51]. According to the second law of thermodynamics, the exergy balance equation is as follows [39,51]:

$$\dot{E}_{D,k} + \dot{E}_{out,k} + \dot{E}_{Q,k} = \dot{E}_{in,k} \tag{16}$$

where $\dot{E}$ represents exergy, $\dot{E}_{D,k}$ represents the exergy destruction rate, $\dot{E}_{out}$ is the output exergy, $\dot{E}_{Q}$ is the heat released by the chemical reaction, $\dot{E}_{in}$ is the input exergy, and the subscript k refers to the component.

Consider the exergy balance of a component, in addition to considering the input and output exergy, the exergy can also be divided into fuel exergy and product exergy. The fuel-product exergy balance equation is as follows [37]:

$$\dot{E}_{F,k} = \dot{E}_{P,k} + \dot{E}_{L,k} + \dot{E}_{D,k} \tag{17}$$

where the subscripts F and P represent the fuel and product, and $\dot{E}_{L,k}$ represent the external exergy destruction rate of the k component. The formula for calculating exergy is as follows:

$$\dot{E}_k = \dot{m}_k \cdot \dot{e}_{x,k} \tag{18}$$

$$\dot{e}_x = (\dot{e}_x)_{ph} + (\dot{e}_x)_{ch} \tag{19}$$

$$(\dot{e}_x)_{ph} = (h - h_0) - T_0 (s - s_0) \tag{20}$$

$$\left(\dot{e}_x\right)_{ch} = \mu_i^* - \mu_{i,o} \tag{21}$$

where $\dot{e}_{x,k}$ represents the specific exergy of component k, $\left(\dot{e}_x\right)_{ph}$ represents the physical specific exergy of component k, $\left(\dot{e}_x\right)_{ch}$ represents the chemical specific exergy of component k, the subscript 0 represents the environmental state, μ_i^* and $\mu_{i,o}$ are the limited state potential and the final dead state potential. Most of the components in the proposed system do not involve chemical reactions and only biomass boilers have combustion reactions. Therefore, the chemical exergy of other components except the biomass boiler is 0. The flue gas emitted from the biomass boiler is a mixed gas. The formula for calculating the chemical exergy of a gas mixture is as follows:

$$\left(\dot{e}_x\right)_{ch,gas\ mixture} = \sum x_i \dot{e}_x\left(T_0, i\right) + RT_0 \sum x_i \ln x_i \tag{22}$$

where x_i represent the molar fraction of the i gas and R is the universal gas constant.

In addition, the exergy of biomass fuel [42] and solar energy [52] is calculated according to the following formula:

$$\dot{E}_{bf} = \beta_{bf} \cdot m_{bf} \cdot LHV_{bf} \tag{23}$$

$$\beta_{bio} = \frac{1.044 + 0.016 \cdot \frac{H}{C} - 0.3493 \cdot \frac{O}{C} \cdot \left(1 + 0.0531 \cdot \frac{O}{C}\right) + 0.0493 \cdot \frac{N}{C}}{1 - 0.4124 \cdot \frac{O}{C}} \tag{24}$$

$$\dot{E}_{sun} = G \times A_{PV/T} \times \left[1 + \frac{1}{3}\left(\frac{T_0}{T}\right)^4 - \frac{4}{3}\frac{T_0}{T}\right] \tag{25}$$

where $\dot{E}_{bf}$, β_{bf}, $\dot{E}_{sun}$ represent biomass fuel exergy, chemical exergy coefficient and solar exergy.

Exergy destruction rate and exergy efficiency are important indicators for evaluating system performance in exergy analysis. Exergy efficiency is the ratio of product exergy and fuel exergy. When external exergy losses are not considered, exergy destruction is the difference between the fuel exergy and the product exergy. Therefore, the magnitude of the exergy efficiency directly reflects the ability of the component fuel to be converted into useful energy. The calculation formulas for the exergy destruction rate and exergy efficiency of each component in the system is shown in Table 3. The calculation formula for exergy efficiency η_{ex} is as follows [53]:

$$\eta_{ex} = \frac{\dot{E}_P}{\dot{E}_F} \tag{26}$$

Table 3 Results of the exergy analysis of the energy system.

Component	$\dot{E}_{D,k}$	$\eta_{ex,k}$
Air preheater	$\dot{E}_{d,AP}=\dot{E}_{13}-\dot{E}_{14}-\dot{E}_{16}+\dot{E}_{15}$	$\frac{\dot{E}_{16}-\dot{E}_{15}}{\dot{E}_{13}-\dot{E}_{14}}$
Biomass boiler	$\dot{E}_{d,bio}=\dot{E}_{bf}+\dot{E}_{16}+\dot{E}_{19}-\dot{E}_{18}-\dot{E}_{13}$	$\frac{\dot{E}_{18}-\dot{E}_{19}}{\dot{E}_{bf}+\dot{E}_{16}-\dot{E}_{13}}$
Condenser 1	$\dot{E}_{d,con1}=\dot{E}_{3}-\dot{E}_{4}-\dot{E}_{24}+\dot{E}_{23}$	$\frac{\dot{E}_{24}-\dot{E}_{23}}{\dot{E}_{3}-\dot{E}_{4}}$
Condenser 2	$\dot{E}_{d,con2}=\dot{E}_{7}-\dot{E}_{8}-\dot{E}_{26}+\dot{E}_{25}$	$\frac{\dot{E}_{26}-\dot{E}_{25}}{\dot{E}_{7}-\dot{E}_{8}}$
Evaporator 1	$\dot{E}_{d,eva1}=\dot{E}_{3}-\dot{E}_{4}+\dot{E}_{8}-\dot{E}_{5}$	$\frac{\dot{E}_{1}-\dot{E}_{5}}{\dot{E}_{18}-\dot{E}_{19}}$
Evaporator 2	$\dot{E}_{d,eva2}=\dot{E}_{6}-\dot{E}_{10}-\dot{E}_{11}+\dot{E}_{12}$	$\frac{\dot{E}_{6}-\dot{E}_{10}}{\dot{E}_{11}-\dot{E}_{12}}$
Preheater	$\dot{E}_{d,pre}=\dot{E}_{2}-\dot{E}_{3}-\dot{E}_{10}+\dot{E}_{9}$	$\frac{\dot{E}_{10}-\dot{E}_{9}}{\dot{E}_{2}-\dot{E}_{3}}$
Pump 1	$\dot{E}_{d,pump1}=\dot{W}_{pump1}-\dot{E}_{5}+\dot{E}_{4}$	$\frac{\dot{E}_{5}-\dot{E}_{4}}{\dot{W}_{pump1}}$
Pump 2	$\dot{E}_{d,pump2}=\dot{W}_{pump2}-\dot{E}_{9}+\dot{E}_{8}$	$\frac{\dot{E}_{9}-\dot{E}_{8}}{\dot{W}_{pump2}}$
PV/T	$\dot{E}_{d,PV/T}=\dot{E}_{12}+\dot{E}_{sun,PV/T}-\dot{E}_{11}-\dot{W}_{PV/T}$	$\frac{\dot{E}_{11}-\dot{E}_{12}+\dot{W}_{PV/T}}{\dot{E}_{sun,PV/T}}$
Turbine 1	$\dot{E}_{d,tur1}=\dot{E}_{1}-\dot{E}_{2}-\dot{W}_{tur1}$	$\frac{\dot{W}_{tur1}}{\dot{E}_{1}-\dot{E}_{2}}$
Turbine 2	$\dot{E}_{d,tur2}=\dot{E}_{6}-\dot{E}_{7}-\dot{W}_{tur2}$	$\frac{\dot{W}_{tur2}}{\dot{E}_{5}-\dot{E}_{6}}$

Note: The subscripts AP, bio, con1, con2, eva1, eva2, pre, tur1 and tur2 represent air preheat, biomass boiler, condenser 1, condenser 2, evaporator 1, evaporator 2, preheater, turbine 1 and turbine 2, respectively.

Conventional exergoeconomic analysis is carried out on the basis of exergy analysis. It can avoid the low economy caused by the pursuit of high exergy efficiency. The exergoeconomic analysis can point out the cost rate caused by exergy destruction and the investment cost of components, and can provide reference for optimizing components from the aspects of economy and efficiency. The exergoeconomic balance equation is as follows [54]:

$$\dot{C}_{out,k}+\dot{C}_{W,k}=\dot{C}_{in,k}+\dot{C}_{Q,k}+\dot{Z}_{k} \tag{27}$$

$$\dot{C}_{k}=c_{k}\dot{E}_{k} \tag{28}$$

$$\dot{Z}_k = \frac{Z_k \cdot CRF}{N} \tag{29}$$

$$CRF = \frac{i_r(1+i_r)^n}{(1+i_r)^n - 1} \tag{30}$$

$$f_{c,k} = \frac{\dot{Z}_k}{\dot{Z}_k + \dot{C}_{D,k} + \dot{C}_{L,k}} \tag{31}$$

where $\dot{C}_{out,k}$ and $\dot{C}_{in,k}$ are the exergoeconomic cost of the output exergy stream and input exergy stream of the component k. $\dot{C}_{w,k}$ and $\dot{C}_{Q,k}$ are the exergoeconomic cost of the output work of component k and the exergoeconomic cost of input component heat. c is the cost per unit exergy of each stream, $\dot{Z}_k$ is the total cost rate related to capital investment, operation and maintenance of the component k, N is the annual operating hours, CRF is the capital recovery factor, i_r is the interest rate, n is the system life, $f_{c,k}$ is the exergoeconomic factor, and $\dot{C}_{D,k}$ is the exergy destruction cost rate.

The cost balance equations and investment cost equations of each component are shown in Table 4.

Table 4 Equations of exergoeconomic analysis for each component [16,55,56].

Component	Cost balance equation	Investment cost equation/$
Air preheater	$\dot{C}_{13} + \dot{C}_{15} + \dot{Z}_{AP} = \dot{C}_{14} + \dot{C}_{16}$	$\dot{Z}_{AP} = 130 \cdot (A_{AP} / 0.093)^{0.78}$
Biomass boiler	$\dot{C}_{19} + \dot{C}_{17} + \dot{C}_{16} + \dot{Z}_{bio} = \dot{C}_{18} + \dot{C}_{13}$	$\dot{Z}_{bio} = 120 \cdot Q_{bio}$
Condenser 1	$\dot{C}_3 + \dot{C}_{23} + \dot{Z}_{con1} = \dot{C}_4 + \dot{C}_{24}$	$\dot{Z}_{con1} = 309.14 \cdot (A_{con1})^{0.85}$
Condenser 2	$\dot{C}_{25} + \dot{C}_8 + \dot{Z}_{con2} = \dot{C}_8 + \dot{C}_{26}$	$\dot{Z}_{con2} = 309.14 \cdot (A_{con2})^{0.85}$
Evaporator 1	$\dot{C}_5 + \dot{C}_{18} + \dot{Z}_{eva1} = \dot{C}_1 + \dot{C}_{19}$	$\dot{Z}_{eva1} = 309.14 \cdot (A_{eva1})^{0.85}$
Evaporator 2	$\dot{C}_{10} + \dot{C}_{11} + \dot{Z}_{eva2} = \dot{C}_{12} + \dot{C}_6$	$\dot{Z}_{eva2} = 309.14 \cdot (A_{eva2})^{0.85}$
Preheater	$\dot{C}_2 + \dot{C}_9 + \dot{Z}_{pre} = \dot{C}_3 + \dot{C}_{10}$	$\dot{Z}_{pre} = 130 \cdot (A_{pre} / 0.093)^{0.78}$
Pump 1	$\dot{C}_4 + \dot{C}_{27} + \dot{Z}_{pump1} = \dot{C}_5$	$\dot{Z}_{pump1} = 3500 \cdot \left(\dot{W}_{pump1}\right)^{0.41}$
Pump 2	$\dot{C}_8 + \dot{C}_{28} + \dot{Z}_{pump1} = \dot{C}_{28}$	$\dot{Z}_{pump2} = 3500 \cdot \left(\dot{W}_{pump2}\right)^{0.41}$
PV/T	$\dot{C}_{12} + \dot{C}_{sun} + \dot{Z}_{PV/T} = \dot{C}_{11} + \dot{C}_{21}$	$\dot{Z}_{PV/T} = 1000 \cdot A_{PV/T}$
Turbine 1	$\dot{C}_1 + \dot{Z}_{tur1} = \dot{C}_2 + \dot{C}_{20}$	$\dot{Z}_{tur1} = 4750 \cdot (\dot{W}_{tur1})^{0.75}$

Turbine 2	$\dot{C}_6 + \dot{Z}_{tur2} = \dot{C}_7 + \dot{C}_{22}$	$\dot{Z}_{tur2} = 4750 \cdot (\dot{W}_{tur})^{0.75}$

Exergoenvironmental analysis is similar to exergoeconomic analysis, and both need to be calculated on the basis of exergy analysis. The main goal of exergoenvironmental analysis is to obtain components with the greatest environmental impact over the life cycle of the system and components with high environmental impact caused by exergy destruction. It can evaluate components with pollutant emissions. Exergoenvironmental analysis balance equation is as follows [20]:

$$\dot{B}_{in,k} + \dot{Y}_k + \dot{B}_k^{PF} = \dot{B}_{out,k} \tag{32}$$

$$\dot{B}_k = \dot{E}_k \cdot b_k \tag{33}$$

$$\dot{Y}_k = \dot{Y}_k^{CO} + \dot{Y}_k^{OM} + \dot{Y}_k^{DI} \tag{34}$$

$$f_{b,k} = \frac{\dot{Y}_k}{\dot{Y}_k + \dot{B}_{D,k}} \tag{35}$$

where $\dot{B}_{in,k}$ and $\dot{B}_{out,k}$ are the environmental impact rate of the output exergy stream and input exergy stream of the component k, $\dot{Y}_k$ is the environmental impact of the component itself, $\dot{B}_k^{PF}$ is the environmental impact rate of pollutants, b_k is the specific environmental impact rate, $\dot{Y}_k^{CO}$, $\dot{Y}_k^{OM}$ and $\dot{Y}_k^{DI}$ are the environmental impact rates generated during the component creation, operation and maintenance and disposal process, $f_{b,k}$ is the exergoenvironmental factor, and $\dot{B}_{D,k}$ is the exergy destruction environmental impact rate. Table 5 shows the exergoenvironmental balance equations and auxiliary equations for each component of the system, and Table 6 shows the environmental impact values of each component of the system.

Table 5 Equation for exergoenvironmental analysis for each component.

Component	Environmental impact balance relation	Auxiliary equation
Air preheater	$\dot{B}_{13} + \dot{B}_{15} + \dot{Y}_{AP} = \dot{B}_{14} + \dot{B}_{16}$	$\dot{B}_{13}/\dot{E}_{13} = \dot{B}_{14}/\dot{E}_{14}$ $\dot{B}_{15} = 0$
Biomass boiler	$\dot{B}_{19} + \dot{B}_{17} + \dot{B}_{16} + \dot{Y}_{bio} = \dot{B}_{18} + \dot{B}_{13}$	$b_{CO_2} = 5.4545 mPt/kg$ $b_{bf} = 0.004889 mPt/kg$ [57]
Condenser 1	$\dot{B}_3 + \dot{B}_{23} + \dot{Y}_{con1} = \dot{B}_4 + \dot{B}_{24}$	$\dot{B}_3/\dot{E}_3 = \dot{B}_4/\dot{E}_4$ $\dot{B}_{23} = 0$

Condenser 2	$\dot{B}_{25}+\dot{B}_{8}+\dot{Y}_{con2}=\dot{B}_{8}+\dot{B}_{26}$	$\dot{B}_{7}/\dot{E}_{7}=\dot{B}_{8}/\dot{E}_{8}$ $\dot{B}_{25}=0$
Evaporator 1	$\dot{B}_{5}+\dot{B}_{18}+\dot{Y}_{eva1}=\dot{B}_{1}+\dot{B}_{19}$	$\dot{B}_{18}/\dot{E}_{18}=\dot{B}_{19}/\dot{E}_{19}$
Evaporator 2	$\dot{B}_{10}+\dot{B}_{11}+\dot{Y}_{eva2}=\dot{B}_{12}+\dot{B}_{6}$	$\dot{B}_{11}/\dot{E}_{11}=\dot{B}_{12}/\dot{E}_{12}$
Preheater	$\dot{B}_{2}+\dot{B}_{9}+\dot{Y}_{pre}=\dot{B}_{3}+\dot{B}_{10}$	$\dot{B}_{3}/\dot{E}_{3}=\dot{B}_{2}/\dot{E}_{2}$
Pump 1	$\dot{B}_{4}+\dot{B}_{27}+\dot{Y}_{pump1}=\dot{B}_{5}$	$\dot{B}_{27}/\dot{E}_{27}=\dot{B}_{20}/\dot{W}_{tur1}$
Pump 2	$\dot{B}_{8}+\dot{B}_{28}+\dot{Y}_{pump1}=\dot{B}_{28}$	$\dot{B}_{28}/\dot{E}_{28}=\dot{B}_{22}/\dot{W}_{tur2}$
PV/T	$\dot{B}_{12}+\dot{B}_{sun}+\dot{Y}_{PV/T}=\dot{B}_{11}+\dot{B}_{21}$	$(\dot{B}_{11}-\dot{B}_{12})/(\dot{E}_{11}-\dot{E}_{12})=\dot{B}_{21}/\dot{W}_{PV/T}$ $\dot{B}_{sun}=0$
Turbine 1	$\dot{B}_{1}+\dot{Y}_{tur1}=\dot{B}_{2}+\dot{B}_{20}$	$\dot{B}_{1}/\dot{E}_{1}=\dot{B}_{2}/\dot{E}_{2}$
Turbine 2	$\dot{B}_{6}+\dot{Y}_{tur2}=\dot{B}_{7}+\dot{B}_{22}$	$\dot{B}_{6}/\dot{E}_{6}=\dot{B}_{7}/\dot{E}_{7}$

Table 6 The environmental impact values of each component of the system [58–60].

Component	Material	Unit component-related environmental impact /mPt/kg			Points/mPt/kg
		Build	Operation and maintenance	Recycle	
Air preheater	Steel(25%), steel high alloy(75%)	704	12.1	-70	646.1
Biomass boiler	Steel(20%), steel high alloy(70%), steel low alloy(10%)	745	20	-70	695
Condenser 1	Steel(100%)	86	12.1	-70	28.1
Condenser 2	Steel(100%)	86	12.1	-70	28.1
Evaporator 1	Steel(100%)	86	12.1	-70	28.1
Evaporator 2	Steel(100%)	86	12.1	-70	28.1
Preheater	Steel(25%), steel high alloy(75%)	704	12.1	-70	646.1
Pump 1	Steel(35%), cast iron(65%)	186	16.9	-70	132.9
Pump 2	Steel(35%), cast iron(65%)	186	16.9	-70	132.9
PV/T	Solar glass(44%), silicon(2%), polyethylene(1%), copper(24%),	639	64	-123	580

	PUR(6%), aluminum(15%), galvanized iron(8%)				
Turbine 1	Steel(25%), steel high alloy(75%)	704	12.1	-70	646.1
Turbine 2	Steel(25%), steel high alloy(75%)	704	12.1	-70	646.1

3.3 Advanced 3E analyses

The difference between advanced exergy analysis and conventional exergy analysis is that advanced exergy analysis divides exergy destruction into endogenous/exogenous, avoidable /unavoidable exergy destruction on the basis of conventional exergy analysis. Through advanced exergy analysis, we can quantitatively analyze the causes of exergy destruction, so that we can judge which exergy destruction of components are worth taking measures to reduce. Endogenous exergy destruction is exergy destruction caused by the component itself. Exogenous exergy destruction is exergy destruction caused by the interaction between components. The sum of these two parts is the exergy destruction of the component under operating conditions [61].

$$\dot{E}_{D,k} = \dot{E}_{D,k}^{EN} + \dot{E}_{D,k}^{EX} \tag{36}$$

where the superscripts EN and EX represent endogenous and exogenous, $\dot{E}_{D,k}^{EN}$ is the endogenous exergy destruction of component k. It is obtained by setting the component k in the model to the real working condition, and the other components are set to operate under ideal working conditions. $\dot{E}_{D,k}^{EX}$ is the exogenous exergy destruction, which is the difference between $\dot{E}_{D,k}$ and $\dot{E}_{D,k}^{EN}$.

Unavoidable exergy destruction is an irreversible loss due to technical limitations. Avoidable exergy destruction is an irreversible loss that can be avoided by technical means. The sum of these two parts is also the exergy destruction of the component under operating conditions [61]:

$$\dot{E}_{D,k} = \dot{E}_{D,k}^{UN} + \dot{E}_{D,k}^{AV} \tag{37}$$

$$\dot{E}_{D,k}^{UN} = \dot{E}_{P,k} \cdot \left(\dot{E}_{D,k} / \dot{E}_{P,k} \right)^{UN} \tag{38}$$

where the superscripts UN and AV represent unavoidable and avoidable. $E_{D,k}^{UN}$ is the unavoidable exergy destruction of component k, which is obtained after the model runs under unavoidable conditions, and $\dot{E}_{D,k}^{AV}$ is the avoidable exergy destruction, which is the difference between $\dot{E}_{D,k}$ and $E_{D,k}^{UN}$.

In addition, the exergy destruction can be further divided to obtain the avoidable endogenous exergy destruction $\dot{E}_{D,k}^{AV,EN}$, the unavoidable endogenous exergy destruction $\dot{E}_{D,k}^{UN,EN}$, the avoidable exogenous exergy destruction $\dot{E}_{D,k}^{AV,EX}$ and the unavoidable exogenous exergy destruction $\dot{E}_{D,k}^{UN,EX}$. Among them, avoidable endogenous exergy destruction is a measure of a component's ability to improve by improving itself. It provides a powerful reference for system optimization. These four exergy destruction can be calculated as follows [61]:

$$\dot{E}_{D,k} = \dot{E}_{D,k}^{UN,EN} + \dot{E}_{D,k}^{AV,EN} + \dot{E}_{D,k}^{UN,EX} + \dot{E}_{D,k}^{AV,EX} \tag{39}$$

$$\dot{E}_{D,k}^{UN,EN} = \dot{E}_{P,k}^{EN} \cdot \left(\dot{E}_{D,k} \big/ \dot{E}_{P,k} \right)^{UN} \tag{40}$$

$$\dot{E}_{D,k}^{AV,EN} = \dot{E}_{D,k}^{EN} - \dot{E}_{D,k}^{UN,EN} \tag{41}$$

$$\dot{E}_{D,k}^{UN,EX} = \dot{E}_{D,k}^{UN} - \dot{E}_{D,k}^{UN,EN} \tag{42}$$

$$\dot{E}_{D,k}^{AV,EX} = \dot{E}_{D,k}^{AV} - \dot{E}_{D,k}^{AV,EN} \tag{43}$$

Advanced exergoeconomic analysis and advanced exergoenvironmental analysis are similar to advanced exergy analysis. It is carried out on the basis of conventional exergoeconomic analysis and conventional exergoenvironmental analysis. The exergy destruction cost rate and exergy destruction environmental impact rate are divided into endogenous/exogenous and avoidable and unavoidable. Advanced exergoeconomic analysis and exergoenvironmental analysis can avoid the high cost and pollution caused by the pursuit of efficient performance. According to the analyses result of the two, the system efficiency, economy and environmental protection can be better balanced. The expressions of the advanced exergy destruction cost rate and exergy destruction environmental impact rate of each component are shown in Table 7. And they satisfy the following relationships:

$$\dot{C}_{D,k} = \dot{C}_{D,k}^{EN} + \dot{C}_{D,k}^{EX} \tag{44}$$

$$\dot{C}_{D,k} = \dot{C}_{D,k}^{UN} + \dot{C}_{D,k}^{AV} \tag{45}$$

$$\dot{C}_{D,k} = \dot{C}_{D,k}^{UN,EN} + \dot{C}_{D,k}^{UN,EX} + \dot{C}_{D,k}^{AV,EN} + \dot{C}_{D,k}^{AV,EX} \tag{46}$$

$$\dot{B}_{D,k} = \dot{B}_{D,k}^{EN} + \dot{B}_{D,k}^{EX} \tag{47}$$

$$\dot{B}_{D,k} = \dot{B}_{D,k}^{UN} + \dot{B}_{D,k}^{AV} \tag{48}$$

$$\dot{B}_{D,k} = \dot{B}_{D,k}^{UN,EN} + \dot{B}_{D,k}^{UN,EX} + \dot{B}_{D,k}^{AV,EN} + \dot{B}_{D,k}^{AV,EX} \tag{49}$$

Table 7 Advanced exergy destruction cost rate and environmental impact rate [62,63].

Type	Exergy destruction cost rate	Exergy destruction environmental impact rate
Endogenous (EN)	$\dot{C}_{D,k}^{EN} = c_{F,k} \cdot \dot{E}_{D,k}^{EN}$	$\dot{B}_{D,k}^{EN} = b_{F,k} \cdot \dot{E}_{D,k}^{EN}$
Exogenous (EX)	$\dot{C}_{D,k}^{EX} = c_{F,k} \cdot \dot{E}_{D,k}^{EX}$	$\dot{B}_{D,k}^{EX} = b_{F,k} \cdot \dot{E}_{D,k}^{EX}$
Avoidable (AV)	$\dot{C}_{D,k}^{AV} = c_{F,k} \cdot \dot{E}_{D,k}^{AV}$	$\dot{B}_{D,k}^{AV} = b_{F,k} \cdot \dot{E}_{D,k}^{AV}$
Unavoidable (UN)	$\dot{C}_{D,k}^{UN} = c_{F,k} \cdot \dot{E}_{D,k}^{UN}$	$\dot{B}_{D,k}^{UN} = b_{F,k} \cdot \dot{E}_{D,k}^{UN}$
Avoidable endogenous (AV,EN)	$\dot{C}_{D,k}^{AV,EN} = c_{F,k} \cdot \dot{E}_{D,k}^{AV,EN}$	$\dot{B}_{D,k}^{AV,EN} = b_{F,k} \cdot \dot{E}_{D,k}^{AV,EN}$
Avoidable exogenous (AV,EX)	$\dot{C}_{D,k}^{AV,EX} = c_{F,k} \cdot \dot{E}_{D,k}^{AV,EX}$	$\dot{B}_{D,k}^{AV,EX} = b_{F,k} \cdot \dot{E}_{D,k}^{AV,EX}$
Unavoidable endogenous (UN,EN)	$\dot{C}_{D,k}^{UN,EN} = c_{F,k} \cdot \dot{E}_{D,k}^{UN,EN}$	$\dot{B}_{D,k}^{UN,EN} = b_{F,k} \cdot \dot{E}_{D,k}^{UN,EN}$
Unavoidable exogenous (UN,EX)	$\dot{C}_{D,k}^{UN,EX} = c_{F,k} \cdot \dot{E}_{D,k}^{UN,EX}$	$\dot{B}_{D,k}^{UN,EX} = b_{F,k} \cdot \dot{E}_{D,k}^{UN,EX}$

4 Results and discussion

This section validates the proposed system. And the results of conventional and advanced exergy, exergoeconomic, and exergoenvironmental analyses of the proposed system are given. The improvement potential of individual components in the system are analyzed.

4.1 Validation

In order to verify the correctness of the established biomass-fired, the ORC model and the PV/T model, the parameters of literature [42] and literature [50] are brought into the established system model. The net power of the system, electrical efficiency were used as the verification objectives and compared with the data in the literatures. The results are shown in Table 8. We observed good agreement between the results obtained in this model and those in the literatures.

Table 8 Comparison of present model results with references.

Parameters	Reference	Present study	Error (%)
ORC[42]			
Organic working medium	R245fa	R245fa	-
Evaporation temperature /K	390	390	-

Condensation temperature /K	326	326	-
Heat source temperature /K	433	433	-
Biomass boiler efficiency /%	90	90	
Power output /kW	256	256.87	0.34
Electrical efficiency /%	8.46	8.56	1.2
PV/T [50]			
Solar radiation intensity (W/m^2)	1000	1000	-
Area of PV/T (m^2)	80	80	-
Temperature coefficient of photovoltaic efficiency (%)	0.5	0.5	-
Power output (kW)	5.82	5.74	-1.33

4.2 Energy analysis

Table 9 shows the input data and energy analysis results of the designed system. R245fa was selected as the working medium for two-stage organic Rankine cycle, and different evaporation temperatures were set for the ORC 1 and the ORC 2 according to the heat source temperatures. The solar radiation intensity of 800W/m^2 was selected, and the basic input data of biomass-fired was set according to the research of Zhu et al. [42]. The energy analysis results show that the designed system can produce 205kW of electricity, and its energy efficiency is 14.14%. Conventional and advanced 3E analyses were performed on the system under these conditions.

Table 9 Input data and energy analysis results.

Parameters	Value
Organic working medium	R245fa
Evaporation temperature of the ORC 1 /K	365.15
Evaporation temperature of the ORC 2 /K	348.15
Condensation temperature of the ORC 1 and ORC 2 /K	313.15
Heat source temperature of the ORC 1 /K	448.15
Biomass boiler efficiency /%	90
Solar radiation intensity (W/m^2)	800
Area of PV/T (m^2)	1000
Cell efficiency (%)	0.32
Power output (kW)	**205**
Energy efficiency (%)	**14.14**

4.3 Conventional 3E analyses

Exergy efficiency and exergy destruction rate are the main criteria to measure the thermodynamic properties of each component. Conventional exergy analysis can obtain the exergy destruction rates and exergy efficiencies of each component, which point the direction for system improvement. Figure 2 shows the proportion of exergy destruction for each component in the proposed system. Among them, evaporator 1 has the highest exergy destruction ($\dot{E}_{D,eva1} = 708.2kW$), accounting for 50.8% of the total exergy destruction of the system. This is followed by the PV/T (25.4%) and evaporator 2 (16.7%). The exergy destruction rates of the air preheater, condenser 1, condenser 2, turbine 1, turbine 2, pump 1, pump 2, and preheater are minimal. The sum of the exergy destruction rates of these components only accounts for 3.1% of the total exergy destruction rate of the system. Therefore, from the perspective of reducing the exergy destruction rate to improve system performance, evaporator 1, the PV/T and evaporator 2 have great potential for improvement.

Figure 3 shows the exergy efficiency of each component in the proposed system. Condenser 1 has the lowest exergy efficiency (1.628%), followed by evaporator 2 (6.712%), condenser 2 (7.121%), air preheater (9.857%), and evaporator 1 (10.96%). Exergy efficiency is the ratio of product exergy to fuel exergy, Table 10 shows the exergy destruction, product exergy and fuel exergy of each component in the system. Although the exergy destruction rate of condenser 1 is small compared to other components, the fuel exergy of the condenser 1 is mostly destroyed, and only a small part is converted into product exergy. Therefore, the exergy efficiency of condenser 1 is low. The reasons for the low exergy efficiency of condenser 2 are similar to those of the condenser 1. Combined with the results of exergy efficiency and exergy destruction rate, evaporator 1 and evaporator 2 have great potential for improvement.

Figure 4 shows the exergy, unit exergy cost, and unit exergy environmental impact of fuel stream and product stream for each component in the system. According to Figure 4(a), the biomass boiler has the highest fuel stream and product stream exergy. And the fuel exergy of biomass boiler is close to the exergy of the product. These indicate that the exergy destruction of the component is small. Therefore, the exergy efficiency of the biomass boiler is higher (93.65%). Secondly, the fuel exergy and product exergy of preheater, turbine 1, turbine 2, pump 1 and pump 2 are also close. Therefore, their exergy efficiencies are also higher, 89.07%, 86.11%, 85.96%, 85.63%, 85.62%, respectively.

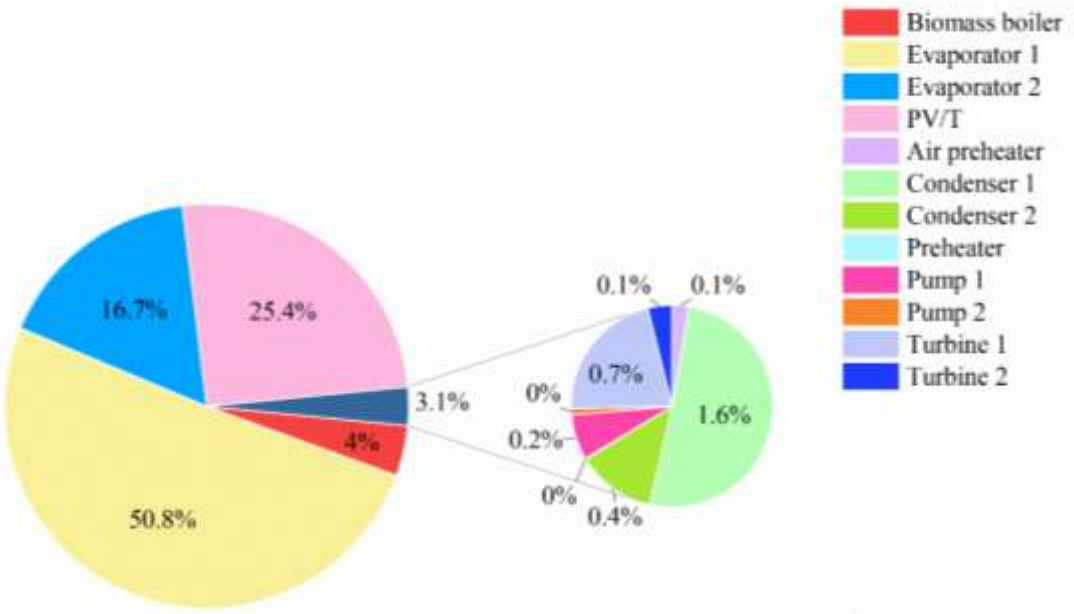

Figure 2 The proportions of exergy destruction of each component.

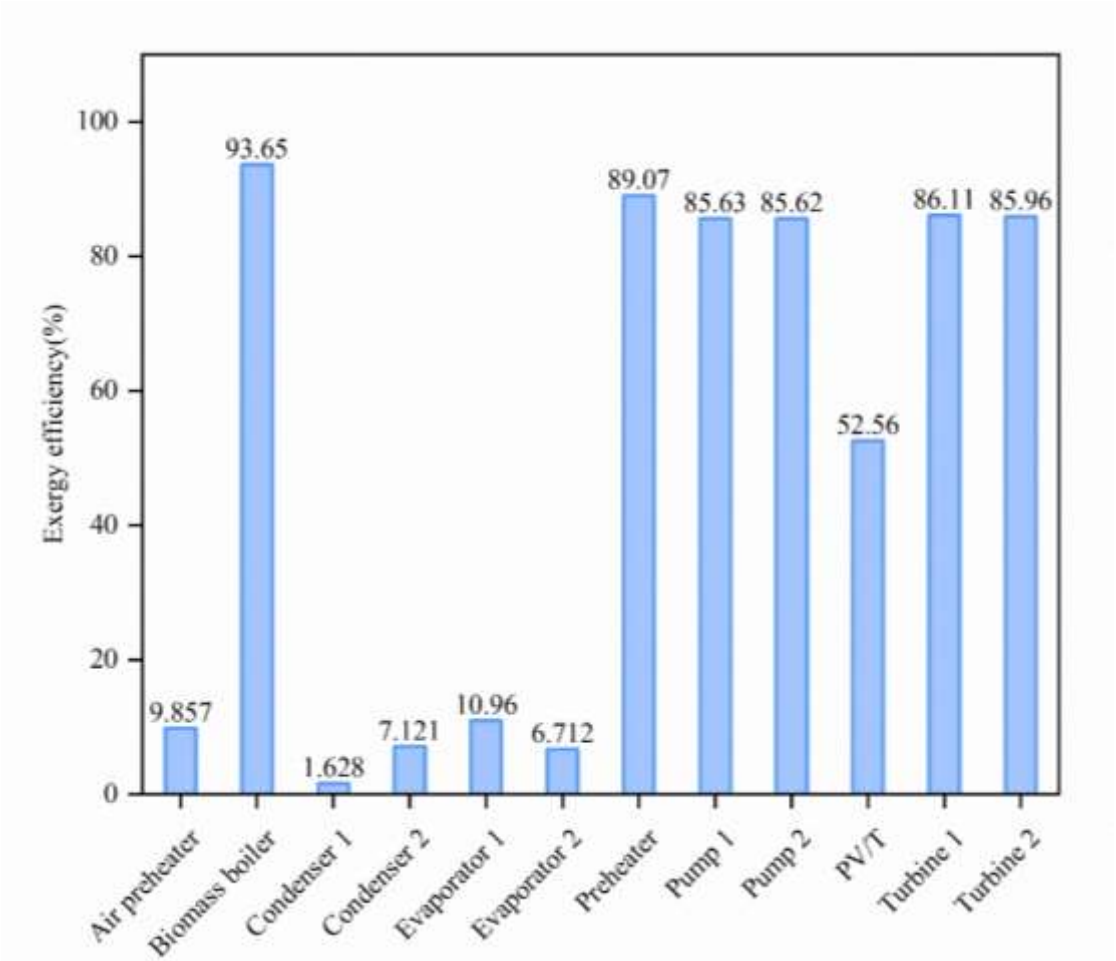

Figure 3 Exergy efficiency of each component.

Table 10 Results of the exergy analysis of the energy system.

Component	$\dot{E}_{D,k}(kW)$	$\dot{E}_{P,k}(kW)$	$\dot{E}_{F,k}(kW)$	$\eta_{ex,k}(\%)$
Air preheater	1.14	1.265	0.1247	9.857
Biomass boiler	56.28	873.931	817.711	93.65
Condenser 1	21.7	0.3591	22.05	1.628
Condenser 2	5.387	0.413	5.8	7.121
Evaporator 1	708.2	795.3	87.17	10.96
Evaporator 2	233.7	250.6	16.82	6.712
Preheater	0.071	0.6471	0.5764	89.07
Pump 1	3.105	1.673	1.432	85.63
Pump 2	0.434	0.2341	0.2004	85.62
PV/T	354.4	747	392.635	52.56
Turbine 1	9.152	65.9	56.75	86.11
Turbine 2	1.656	11.79	10.14	85.96

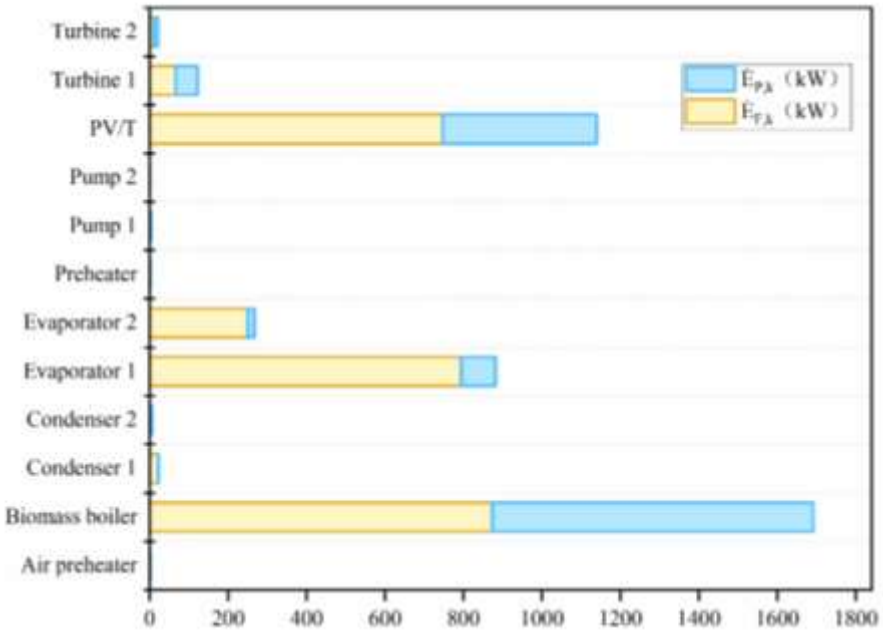

(a)

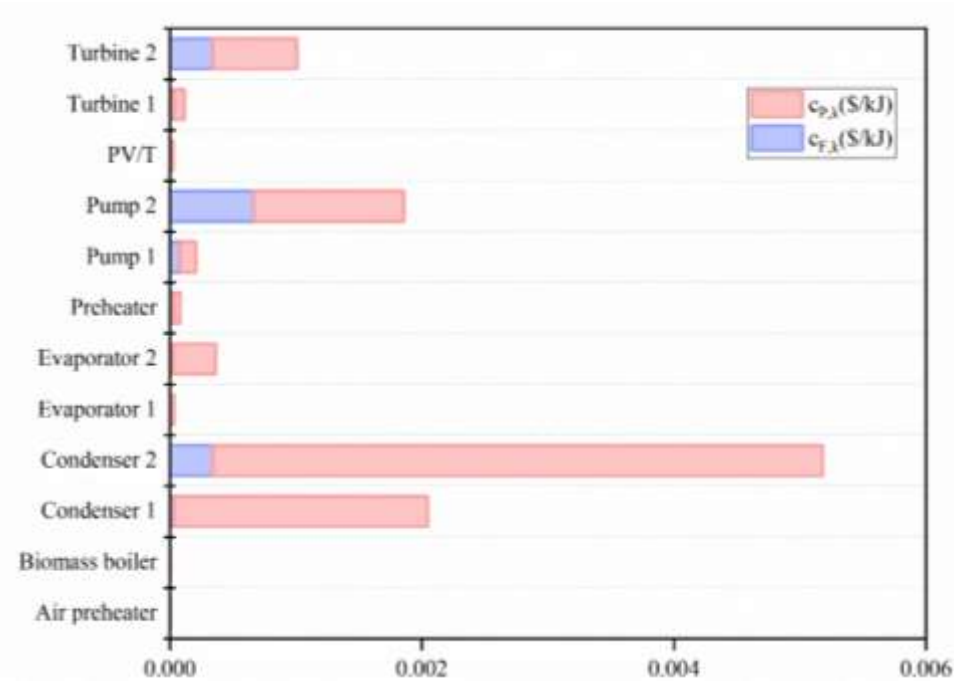

(b)

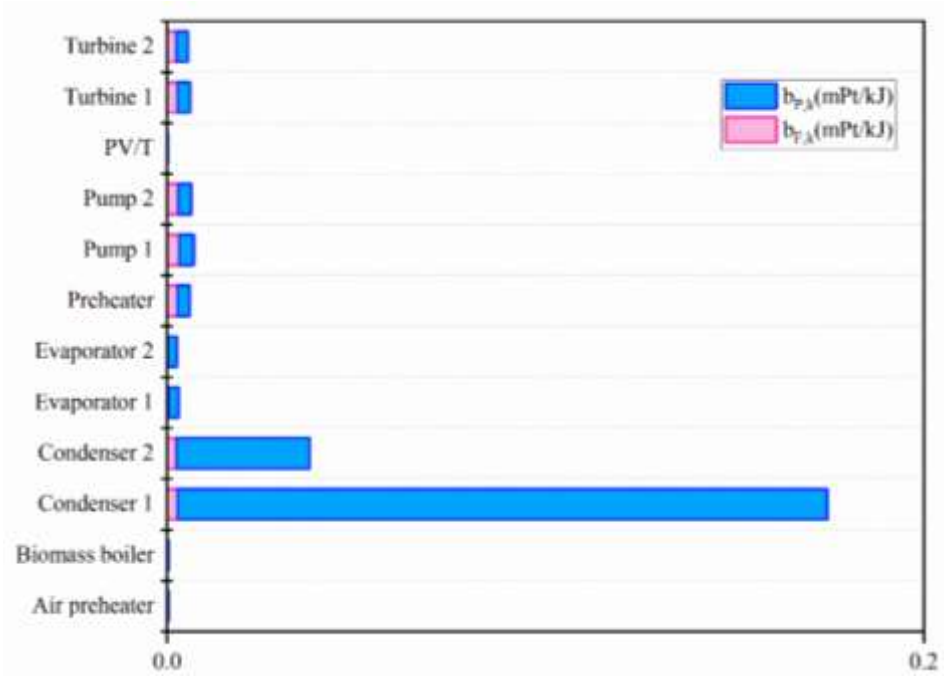

(c)

Figure 4 (a) Exergy of the fuel and product, (b) Cost of fuel and product, (c) Environmental impacts of fuel and product streams of components.

Table 11 presents the results of conventional exergoeconomic analysis. Figure 5-6 show the exergy destruction cost rates and investment cost rates of each component. Obviously, evaporator 2 has the highest exergy destruction cost rate, followed by evaporator 1 and

condenser 2, which the exergy destruction cost rates are 19.15$/h, 8.477$/h and 6.609$/h. Exergy destruction is an important factor affecting the exergy destruction cost rate. According to Figure 4(a), most of the fuel exergy of evaporator 2 and evaporator 1 are lost, and only a small part is converted into product exergy. Therefore, the exergy destruction cost rates of these components are high. The exergy destruction cost rate of the remaining components are low, and the exergy destruction cost rate of the PV/T is 0$/h. This is because solar energy as a free fuel supplies the PV/T, so that the fuel stream cost for the PV/T is 0. According to the formula Eq (28), the exergy destruction cost rate of the PV/T is calculated to be 0.

Table 11 shows the exergoeconomic factors for each component of the system. The exergoeconomic factors reflect the relationship between component efficiency and economy. The PV/T has the highest exergoeconomic factor, and its value is 1. This is due to the fact that solar energy is free. Therefore, the economic evaluation of the PV/T can only start from the investment cost of the component itself. Secondly, turbine 1 (89.5%), turbine 2 (82.96%), and preheater (81.1%) have a higher exergoeconomic factor. These show that the investment cost rate of these components is high, but their exergy destruction cost rate is low. Therefore, the investment cost rates of these components can be appropriately reduced to obtain better economy. In addition, the exergoeconomic factors of the remaining components are less than 50%. Among them, condenser 1 (2.28%), condenser 2 (1.25%), evaporator 1 (0.44%), evaporator 2 (0.45%) have an exergoeconomic factor of less than 1%. It is due to the high exergy destruction cost rates of these four components. Therefore, it is possible to consider sacrificing some of the economy to improve the performance of these four components.

Figure 4(b) shows unit fuel stream cost and unit product stream cost. It's not hard to see that condenser 2 has the highest unit exergy cost associated with both input and output streams. Among them, output stream of condenser 2 has the highest unit product exergy cost, followed by condenser 1, pump 2 and turbine 2, which are 0.0048$/kJ, 0.002$/kJ, 0.0012$/kJ and 0.00067$/kJ. Therefore, from the aspect of reducing the unit exergy cost of product stream, condenser 2, condenser 1, pump 2 and turbine 2 can be optimized to improve the economy of the system.

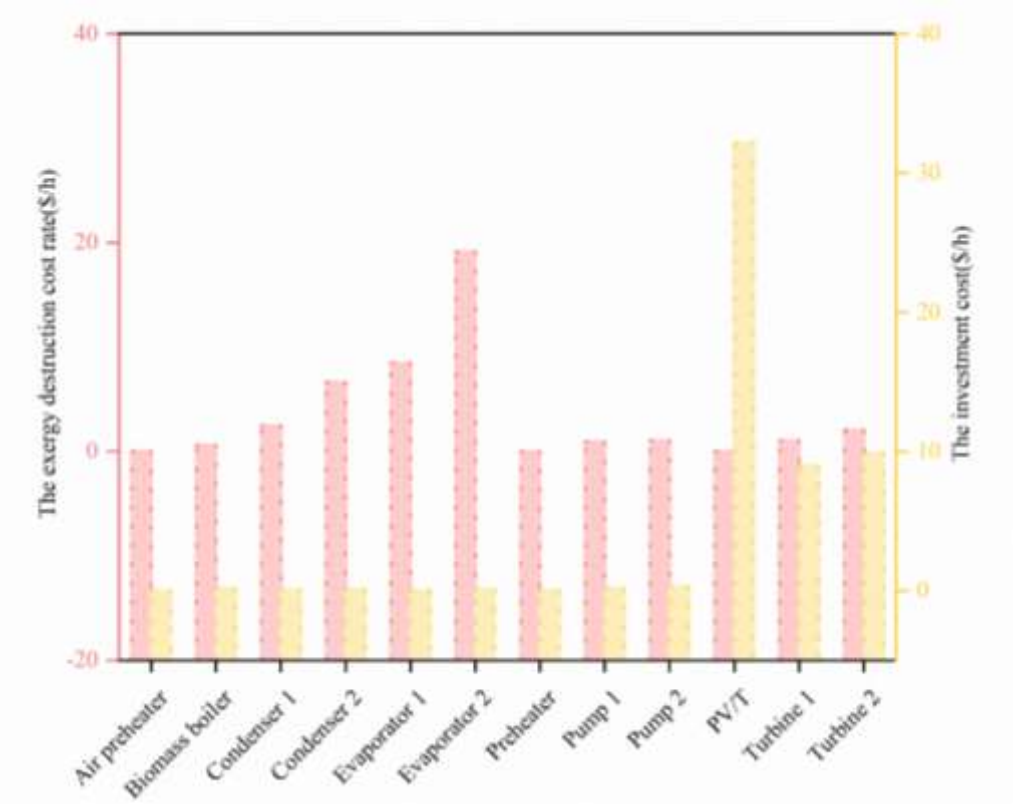

Figure 5 The exergy destruction cost rate and investment cost.

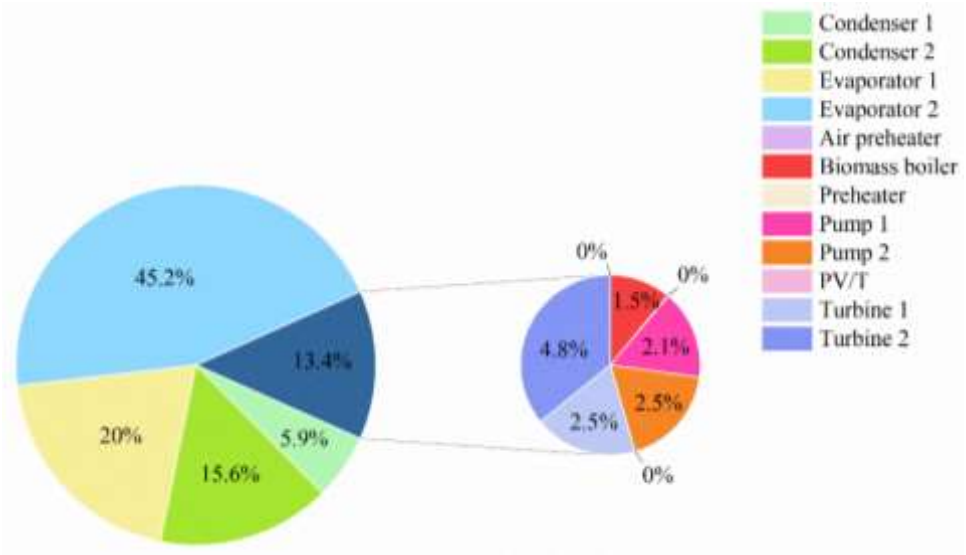

Figure 6 The proportions of exergy destruction cost of each component.

Table 11 Results of the exergoeconomic analysis of the energy system.

Component	$\dot{E}_{D,k}(kW)$	$c_{F,k}(\$/kJ)$	$c_{P,k}(\$/kJ)$	$\dot{C}_{D,k}(\$/h)$	$\dot{Z}_k(\$/h)$	$\dot{C}_{D,k}+\dot{Z}_k(\$/h)$	$f_k(\%)$
Air preheater	1.14	0.36×10^{-6}	0.33×10^{-5}	0.0015	0.00016	0.00166	9.866
Biomass	56.28	0.31×10^{-5}	0.33×10^{-5}	0.6212	0.1482	0.7694	19.26

boiler							
Condenser 1	21.7	0.32×10^{-4}	0.2×10^{-2}	2.501	0.0584	2.5594	2.28
Condenser 2	5.387	0.34×10^{-3}	0.48×10^{-2}	6.609	0.0836	6.6926	1.25
Evaporator 1	708.2	0.33×10^{-5}	0.30×10^{-4}	8.477	0.0378	8.5148	0.44
Evaporator 2	233.7	0.23×10^{-4}	0.34×10^{-3}	19.15	0.0862	19.2362	0.45
Preheater	0.071	0.32×10^{-4}	0.53×10^{-4}	0.0082	0.035	0.0432	81.1
Pump 1	3.105	0.81×10^{-4}	0.13×10^{-3}	0.9078	0.166	1.0738	15.43
Pump 2	0.434	0.67×10^{-3}	0.12×10^{-2}	1.044	0.296	1.34	22.09
PV/T	354.4	0	0.23×10^{-4}	0	32.18	32.18	1
Turbine 1	9.152	0.32×10^{-4}	0.81×10^{-4}	1.055	8.995	10.05	89.5
Turbine 2	1.656	0.34×10^{-3}	0.67×10^{-3}	2.031	9.888	11.919	82.96

Table 12 presents the results of a conventional exergoenvironmental analysis. Figure 7-8 show the exergy destruction environmental impact rate and the component-related environmental impact rate. Evaporator 1 has the highest exergy destruction environmental impact rate (775.3mPt/h), followed by condenser 1 (218.4mPt/h), which accounted for 58.29%, and 16.42% of the total exergy destruction environmental impact rate, respectively. The exergy destruction environmental impact rate of the remaining components is low. Among them, the environmental impact rate of the PV/T is 0mPt/h. This is because solar energy is used as a fuel for the PV/T. Solar energy has no environmental impact, so that the fuel stream environmental impact of the PV/T is 0. According to the formula Eq (33), the exergy destruction environmental impact rate of the PV/T is 0.

Table 12 shows the exergoenvironmental factors for each component of the system. The exergoenvironmental factors reflect the relationship between component efficiency and environmental performance. The PV/T has the highest exergoenvironmental factor, which has a value of 1. This is due to the fact that solar energy has no environmental impact. Therefore, the environmental assessment of the PV/T can only start from the component-related environmental impact. Secondly, the exergoenvironmental factor of biomass boiler is also very high (99.94%), indicating that the environmental impact rate of the boiler-related is high. Therefore, it is necessary to consider reducing the component-related environmental impact to improve the environmental performance of the system. However, the exergoenvironmental factors of the other components are less than 15%. It shows that the exergy destruction

environmental impact rates of these components are high, while the component-related environmental impact rates are low. Therefore, the efficiency of these components can be appropriately improved to reduce the environmental impact caused by exergy destruction. Among them, condenser 1, condenser 2, evaporator 1, pump 1, pump 2 have exergoenvironmental factor of less than 1%. Therefore, these components can be prioritized the environmental performance of these components to reduce the exergy destruction environmental impact.

Figure 4(c) shows the unit fuel stream environmental impact and unit product stream environmental impact. It is clear that the condenser 1 (0.1717) and condenser 2 (0.0352) have a large unit product stream environmental impact. Therefore, optimizing condenser 1 and condenser 2 can improve the environmental performance of the system by reducing the unit product stream environmental impact.

Table 12 Results of the exergoenvironmental analysis of the system.

Component	$\dot{E}_{D,k}(kW)$	$b_{F,k}(mPt/kJ)$	$b_{P,k}(mPt/kJ)$	$\dot{B}_{D,k}(mPt/h)$	$\dot{Y}_k(mPt/h)$	$\dot{B}_{D,k}+\dot{Y}_k(mPt/h)$	$f_k^*(\%)$
Air preheater	1.14	0.30×10^{-4}	0.30×10^{-3}	0.1243	0.0014	0.1257	1.15
Biomass boiler	56.28	0.21×10^{-6}	0.30×10^{-3}	0.043	77.91	77.953	99.94
Condenser 1	21.7	0.0028	0.1717	218.4	0.0062	218.4062	2.84×10^{-3}
Condenser 2	5.387	0.0025	0.0352	48.65	0.0067	48.6567	0.014
Evaporator 1	708.2	0.30×10^{-3}	0.0028	775.3	1.552	776.852	0.2
Evaporator 2	233.7	0.16×10^{-3}	0.0025	137.6	2.293	139.893	1.6
Preheater	0.071	0.0028	0.0032	0.712	0.0415	0.7535	5.5
Pump 1	3.105	0.0033	0.0038	36.42	0.0075	36.4275	0.02
Pump 2	0.434	0.003	0.0035	4.673	0.0047	4.6777	0.1
PV/T	354.4	0	0.16×10^{-3}	0	231.2	231.2	1
Turbine 1	9.152	0.0028	0.0033	93.13	2.225	95.355	2.36
Turbine 2	1.656	0.0025	0.003	14.95	2.532	17.482	14.48

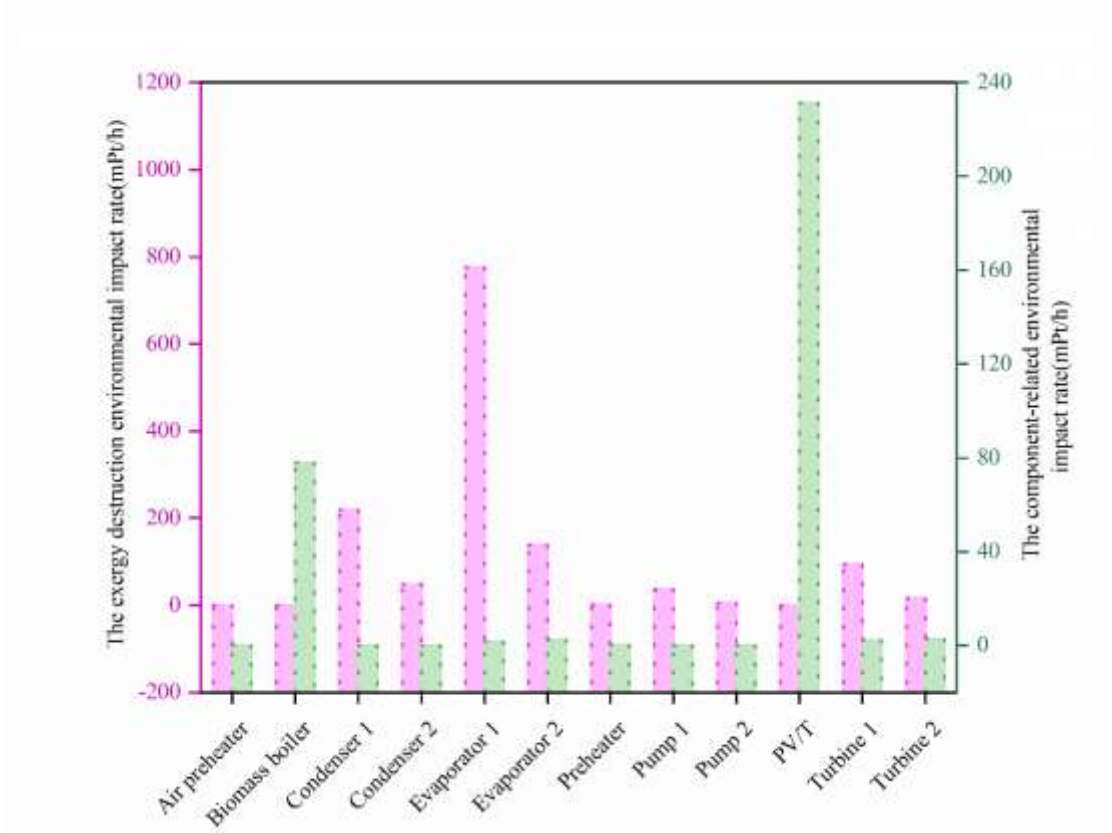

Figure 7 The exergy destruction environmental impact rate and component-related environmental impact rate.

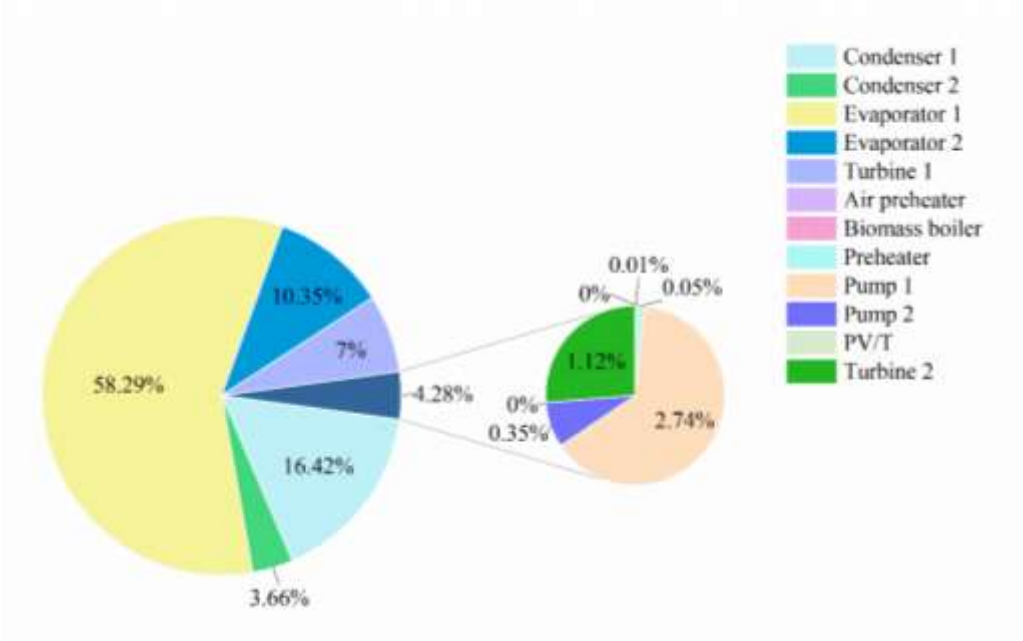

Figure 8 The proportion of exergy destruction environmental impact of each component.

4.4 Advanced 3E analyses

Conventional 3E analyses indicate the components that need to be improved, but do not indicate the extent to which the component can be improved. According to the model output under real working conditions, ideal working conditions and unavoidable working conditions, advanced 3E analyses can divide the exergy destruction rate, exergy destruction cost rate and exergy destruction environmental impact rate into endogenous/exogenous and avoidable/unavoidable. Among them, the avoidable endogenous exergy destruction rate, exergy destruction cost rate and exergy destruction environmental impact rate are the key focus objects. They represent the ability to reduce the exergy destruction rate, exergy destruction cost rate and exergy destruction environmental impact rate by adjusting technical constraints and component efficiency.

It can be seen from Table 13 that except for the evaporator 2 and preheater, the endogenous exergy destruction rates of other components are higher than that of exogenous exergy destruction. The total endogenous exergy destruction of the system accounted for 93.2% of the total exergy destruction. This shows that most of the exergy destruction of the system is caused by the inefficiency of the components themselves. So the energy system can be improved by increasing the efficiency of the components themselves. For evaporator 2 and preheater whose exogenous exergy destruction are greater than that of endogenous exergy destruction, so exergy destruction of evaporator 2 and preheater can be reduced by improving the components associated with them. At the same time, the avoidable exergy destruction of the system according to Table 13 accounts for 7.95% of the total exergy destruction, which indicates that the avoidable exergy destruction rate of the system is small. However, evaporator 1 and the PV/T have a high of avoidable exergy destruction ($\dot{E}_{D,eva1}^{AV} = 136.9kW$, $\dot{E}_{D,PV/T}^{AV} = 120.6kW$), so they are another direction to improve the system. In addition, avoidable exergy destruction of condenser 1, condenser 2, preheater, turbine 1 and turbine 2 are greater than unavoidable exergy destruction. Therefore, these components have better potential for improvement. In addition to the above components, the avoidable exergy destruction of other components is less than the unavoidable exergy destruction. Therefore, improvements to these components will not have a large impact on the system.

Avoidable endogenous exergy destruction in the system represents the ability to reduce exergy destruction by improving component efficiency and improving technical conditions. Among them, the avoidable endogenous exergy destruction of evaporator 1 and the PV/T are high. Therefore, they have a high space to reduce exergy destruction by improving technical conditions and increasing their own efficiency. In addition, the avoidable endogenous exergy destruction of air preheater, biomass boiler, condenser 1, condenser 2, pump 1, pump 2, turbine

1, turbine 2 are greater than exogenous avoidable exergy destruction, indicating that these components also have certain improvement potential in their own efficiency and technical limitations.

Table 13 Results of advanced exergy analysis for the proposed system.

Component	$\dot{E}_{D,k}(kW)$	$\dot{E}_{D,k}^{EN}(kW)$	$\dot{E}_{D,k}^{EX}(kW)$	$\dot{E}_{D,k}^{AV}(kW)$	$\dot{E}_{D,k}^{UN}(kW)$	$\dot{E}_{D,k}^{UN}(kW)$		$\dot{E}_{D,k}^{AV}(kW)$	
						$\dot{E}_{D,k}^{UN,EN}(kW)$	$\dot{E}_{D,k}^{UN,EX}(kW)$	$\dot{E}_{D,k}^{AV,EN}(kW)$	$\dot{E}_{D,k}^{AV,EX}(kW)$
Air preheater	1.14	1.14	0	0.172	0.9648	0.9646	0.0002579	0.1754	-0.0002579
Biomass boiler	56.28	195.8	-139.5	-175.9	232.2	192.8	39.33	2.93	-178.8
Condenser 1	21.7	20.97	0.7297	20.18	1.518	1.491	0.02672	19.48	0.703
Condenser 2	5.387	3.593	1.794	4.143	1.245	0.8396	0.405	2.753	1.389
Evaporator 1	708.2	707.7	0.4336	136.9	571.3	571.1	0.1966	136.6	0.237
Evaporator 2	233.7	3.004	230.7	-2.967	236.7	114.4	122.3	-111.4	108.4
Preheater	0.071	0.0242	0.0465	0.04994	0.02078	14.16	-14.14	-14.13	14.18
Pump 1	3.105	3.105	0	0.1689	2.936	2.937	-0.0004556	0.1685	0.0004556
Pump 2	0.434	0.2969	0.1375	0.02355	0.4109	0.2807	0.1302	0.01622	0.007337
PV/T	354.4	354.4	0	120.6	233.8	233.8	0.0001849	120.6	-0.0001849
Turbine 1	9.152	9.148	0.0039	6.412	2.74	3.18	-0.4403	5.968	0.4442
Turbine 2	1.656	1.131	0.5244	1.16	0.4951	0.3934	0.1016	0.7377	0.4228

Table 14 shows the endogenous/exogenous and avoidable/unavoidable exergy destruction cost rates for each component of the system. It can be seen that except for evaporator 2 and preheater, the endogenous exergy destruction cost rates of other components are higher than that of exogenous exergy destruction cost rates. It shows that the exergy destruction cost rates of these components are greatly affected by irreversibility. Moreover, the interaction between components has little impact on exergy destruction cost rate of the system. Therefore, in addition to the evaporator 2 and preheater, other components can be improved in their own efficiency. For the avoidable and unavoidable exergy destruction cost rate, except for condenser 1, condenser 2, preheater, turbine 1, turbine 2, the unavoidable exergy destruction cost rates of other components are greater than the avoidable exergy destruction cost rates. In addition, based on the calculation results of the avoidable endogenous exergy destruction cost rate, the

avoidable endogenous exergy destruction cost rates of air preheater, biomass boiler, condenser 1, condenser 2, evaporator 1, pump 1, pump 2, turbine 1 and turbine 2 are greater than the avoidable exogenous exergy destruction cost rates. Therefore, it is worth improving the efficiency of the components themselves to reduce the exergy destruction cost rate. Finally, the condenser 2 has the highest avoidable endogenous exergy destruction cost rate ($\dot{C}_{D,con2}^{AV,EN} = 3.377\$/h$), so it has the highest potential for improvement. This is followed by the condenser 1 ($\dot{C}_{D,con1}^{AV,EN} = 2.246\$/h$).

Table 14 Results of advanced exergoeconomic analysis for the proposed system.

Component	$\dot{C}_{D,k}(\$/h)$	$\dot{C}_{D,k}^{EN}(\$/h)$	$\dot{C}_{D,k}^{EX}(\$/h)$	$\dot{C}_{D,k}^{AV}(\$/h)$	$\dot{C}_{D,k}^{UN}(\$/h)$	$\dot{C}_{D,k}^{UN}(\$/h)$		$\dot{C}_{D,k}^{AV}(\$/h)$	
						$\dot{C}_{D,k}^{UN,EN}(\$/h)$	$\dot{C}_{D,k}^{UN,EX}(\$/h)$	$\dot{C}_{D,k}^{AV,EN}(\$/h)$	$\dot{C}_{D,k}^{AV,EX}(\$/h)$
Air preheater	0.0015	0.0015	0	0.0002294	0.0013	0.001263	3.376E-07	0.0002296	-0.2×10^{-6}
Biomass boiler	0.6212	2.163	-1.541	-1.943	2.566	2.13	0.4345	0.03237	-1.976
Condenser 1	2.501	2.417	0.08412	2.326	0.175	0.1719	0.00308	2.246	0.08104
Condenser 2	6.609	4.408	2.201	5.083	1.527	1.03	0.4969	3.377	1.704
Evaporator 1	8.477	8.472	0.0052	1.639	6.839	6.837	0.002353	1.635	0.002837
Evaporator 2	19.15	0.2462	18.9	-0.2431	19.4	9.374	10.02	-9.128	8.882
Preheater	0.0082	0.0028	0.0054	0.005757	0.0024	1.632	-1.63	-1.629	1.635
Pump 1	0.9078	0.9078	0	0.04938	0.8584	0.8587	-0.000133	0.04927	0.0001332
Pump 2	1.044	0. 7132	0.3303	0.05657	0.9871	0.6743	-0.3128	0.03897	0.01763
PV/T	0	0	0	0	0	0	0	0	0
Turbine 1	1.055	1.055	0.0004	0.7391	0.3159	0.3666	-0.05076	0.688	0.05121
Turbine 2	2.031	1.388	0.6433	1.423	0.6074	0.4826	0.1246	0.905	0.5187

Table 15 shows the endogenous/exogenous and avoidable/unavoidable exergy destruction environmental impact rates for each component of the system. It can be seen that the

endogenous exergy destruction environmental impact rates of most components are higher than exogenous exergy destruction environmental impact rates of that. Only evaporator 2 and preheater have a greater exogenous exergy destruction environmental impact rate. These show that in addition to evaporator 2 and preheater, other components have high potential to improve in their own efficiency. These also show that the evaporator 2 and preheater have a strong correlation with other components. Therefore, improving the components related to evaporator 2 and preheater is conducive to reducing the exergy destruction environmental impact rate. For the avoidable and unavoidable exergy destruction environmental impact rate, except for condenser 1, condenser 2, turbine 1, turbine 2, the unavoidable exergy destruction environmental impact rates of other components are greater than the avoidable exergy destruction environmental impact rate. Finally, based on the calculation results of the avoidable endogenous exergy destruction environmental impact rate, condenser 1 has the highest avoidable endogenous exergy destruction environmental impact rate ($\dot{B}_{D,con1}^{AV,EN}=196.1 mPt/h$), so it has the highest improvement potential. This is followed by evaporator 1 and turbine 1 ($\dot{B}_{D,eva1}^{AV,EN}=149.6 mPt/h$, $\dot{B}_{D,tur1}^{AV,EN}=60.08 mPt/h$).

Table 15 Results of advanced exergoenvironmental analysis for the proposed system.

Component	$\dot{B}_{D,k}(mPt/h)$	$\dot{B}_{D,k}^{EN}(mPt/h)$	$\dot{B}_{D,k}^{EX}(mPt/h)$	$\dot{B}_{D,k}^{AV}(mPt/h)$	$\dot{B}_{D,k}^{UN}(mPt/h)$	$\dot{B}_{D,k}^{UN}(mPt/h)$		$\dot{B}_{D,k}^{AV}(mPt/h)$	
						$\dot{B}_{D,k}^{UN,EN}(mPt/h)$	$\dot{B}_{D,k}^{UN,EX}(mPt/h)$	$\dot{B}_{D,k}^{AV,EN}(mPt/h)$	$\dot{B}_{D,k}^{AV,EX}(mPt/h)$
Air preheater	0.1243	0.1243	0	0.01911	0.1052	0.1052	0.000028	0.01913	-0.000028
Biomass boiler	0.043	0.1493	-0.1064	-0.1341	0.177	0.147	0.02999	0.002234	-0.1363
Condenser 1	218.4	211.1	7.346	203.2	15.28	15.01	0.269	196.1	7.077
Condenser 2	48.65	32.44	16.2	37.41	11.24	7.582	3.657	24.86	12.54
Evaporator 1	775.3	774.8	0.4747	149.9	625.5	625.3	0.2152	149.6	0.2595
Evaporator 2	137.6	1.768	135.8	-1.747	139.3	67.35	72	-65.58	63.82
Preheater	0.712	0.2436	0.4681	0.5028	0.2092	142.6	-142.4	-142.2	142.8

Pump 1	36.42	36.42	0	1.981	34.44	34.45	-0.005344	1.977	0.005344
Pump 2	4.673	3.193	1.479	0.2533	4.419	3.019	-1.4	0.1744	0.0789
PV/T	0	0	0	0	0	0	0	0	0
Turbine 1	92.13	92.1	0.03926	64.55	27.58	32.01	-4.433	60.08	4.472
Turbine 2	14.95	10.21	4.735	10.47	4.471	3.552	0.9174	6.661	3.818

Key results of conventional and advanced 3E analyses are presented in Table 16. Conventional 3E analyses can obtain exergy destruction rates, exergy destruction cost rates and exergy destruction environmental impact rates of each component in the system. Advanced 3E analyses divide the results from conventional 3E analyses, and then obtains the key results: avoidable endogenous exergy destruction rates, exergy destruction cost rates and exergy destruction environmental impact rates. Exergy destruction rates, exergy destruction cost rates and exergy destruction environmental impact rates represent the ability to reduce them by improving the component's own performance and improving working conditions. As a result, they are better able to prioritize component. According to Table 16, conventional exergy analysis pointed out that evaporator 1, the PV/T and evaporator 2 have a high exergy destruction rate, so they become main goals to reduce the exergy destruction and improve system performance. But advanced exergy analysis pointed out that the avoidable endogenous exergy destruction rate of evaporator 2 is negative, so it basically does not have the ability to optimize by adjusting its own performances and working conditions, and its exergy destruction rate is affected by the complex structure of the system. Meanwhile, the avoidable endogenous exergy destruction rate of condenser 1 and turbine 1 are 89.77% and 65.21% of their total. These indicate that these two components have excellent improvement potential in reducing exergy destruction. In addition, the optimization opinions obtained by advanced exergoeconomic analysis and advanced exergoenvironmental analysis are also different from those obtained by conventional exergoeconomic analysis and conventional exergoenvironmental analysis. This means that components with a high exergy destruction rate, exergy destruction cost rate and exergy destruction environmental impact rate do not necessarily have the best improvement potential, and so detailed advanced 3E analyses are required before actual optimization operations.

Table 16 Key results of conventional and advanced 3E analyses.

Component	$\dot{E}_{D,k}(kW)$	$\dot{E}_{D,k}^{AV,EN}(kW)$	$\dot{C}_{D,k}(\$/h)$	$\dot{C}_{D,k}^{AV,EN}(\$/h)$	$\dot{B}_{D,k}(mPt/h)$	$\dot{B}_{D,k}^{AV,EN}(mPt/h)$
Air preheater	1.14	0.1754	0.0015	0.0002296	0.1243	0.01913
Biomass boiler	56.28	2.93	0.6212	0.03237	0.043	0.002234
Condenser 1	21.7	19.48	2.501	2.246	218.4	196.1
Condenser 2	5.387	2.753	6.609	3.377	48.65	24.86
Evaporator 1	708.2	136.6	8.477	1.635	775.3	149.6
Evaporator 2	233.7	-111.4	19.15	-9.128	137.6	-65.58
Preheater	0.071	-14.13	0.0082	-1.629	0.712	-142.2
Pump 1	3.105	0.1685	0.9078	0.04927	36.42	1.977
Pump 2	0.434	0.01622	1.044	0.03897	4.673	0.1744
PV/T	354.4	120.6	0	0	0	0
Turbine 1	9.152	5.968	1.055	0.688	92.13	60.08
Turbine 2	1.656	0.7377	2.031	0.905	14.95	6.661

5 Conclusion

In this study, an energy system coupled with biomass, solar energy and two-stage ORC is proposed. The stable energy output of biomass energy is used to compensate for the fluctuation of solar modules. Biomass energy provides heat to the ORC 1 to drive turbine 1 to do work and generate electricity. The expanded working fluid is fed into the preheater and then the working fluid of the ORC 2 is preheated. In this way, it compensates for the defect of the ORC 2 operation fluctuation caused by the low heat output of the PV/T when the solar radiation is not strong. In addition, conventional and advanced 3E analyses of the energy system were carried out. Conventional 3E analyses show that evaporator 1 has the highest exergy destruction rate and exergy destruction environmental impact rate, and evaporator 2 has the highest exergy destruction cost rate. Therefore, according to the conventional 3E analyses, evaporator 1 and evaporator 2 should be the priority components for improvement. However, advanced 3E analyses show that avoidable endogenous exergy destruction /cost/environmental impact rate

of evaporator 2 is negative. This shows that it basically does not have the potential to improve by improving its own efficiency and working conditions. Meanwhile, evaporator 1 has the highest avoidable endogenous exergy destruction and avoidable endogenous exergy destruction environmental impact rate, condenser 2 has the highest avoidable endogenous exergy destruction cost rate. These indicate that evaporator 1 and condenser 2 should be prioritized for optimization.

The results show that improving evaporator 1 and condenser 2 are effective and reasonable means to optimize the proposed system. However, conventional and advanced 3E analyses were only performed based on simulation results in this study. In future work, conventional and advanced 3E analyses are performed based on experimental data should be emphasized. In addition, it is also necessary to focus on the improvement of evaporators and condensers, including selecting appropriate models, designing reasonable parameters and optimizing working conditions.

Declaration of competing interest

The authors declare that they have no known competing financial interests or personal relationships that could have appeared to influence the work reported in this paper.

Acknowledgement

This work was financially supported by the Opole University of Technology as part of the GRAS project no. 270/23. The research leading to these results has received funding from the Norwegian Financial Mechanism 2014-2021 under Project Contract No 2020/37/K/ST8/02748.

Reference

[1] J. Oyekale, E. Emagbetere, Comparative design-point and yearly advanced exergoenvironmental analyses of a solar-biomass organic Rankine cycle power plant, Energy Sources, Part A: Recovery, Utilization, and Environmental Effects. 44 (2022) 10433–10449. https://doi.org/10.1080/15567036.2022.2150795.

[2] X. Qi, J. Wang, G. Królczyk, P. Gardoni, Z. Li, Sustainability analysis of a hybrid renewable power system with battery storage for islands application, Journal of Energy Storage. 50 (2022) 104682. https://doi.org/10.1016/j.est.2022.104682.

[3] Y.A. Situmorang, Z. Zhao, A. Yoshida, A. Abudula, G. Guan, Small-scale biomass gasification systems for power generation (<200 kW class): A review, Renewable and Sustainable Energy Reviews. 117 (2020) 109486. https://doi.org/10.1016/j.rser.2019.109486.

[4] S. Masoud Parsa, A. Yazdani, H. Aberoumand, Y. Farhadi, A. Ansari, S. Aberoumand, N. Karimi, M. Afrand, G. Cheraghian, H. Muhammad Ali, A critical analysis on the energy and exergy performance of photovoltaic/thermal (PV/T) system: The role of nanofluids stability and synthesizing method, Sustainable Energy Technologies and Assessments. 51 (2022) 101887. https://doi.org/10.1016/j.seta.2021.101887.

[5] A. Suzuki, S. Kitamura, Combined Photovoltaic and Thermal Hybrid Collector, Jpn. J. Appl. Phys. 19 (1980) 79. https://doi.org/10.7567/JJAPS.19S2.79.

[6] L. Ma, Z. Tang, C. Wang, Y. Sun, X. Lv, Y. Chen, Research Status and Future Development Strategy of Biomass Energy, Bulletin of Chinese Academy of Sciences. 34 (2019) 434–442. https://doi.org/10.16418/j.issn.1000-3045.2019.04.008.

[7] M. Jordan, V. Lenz, M. Millinger, K. Oehmichen, D. Thrän, Future competitive bioenergy technologies in the German heat sector: Findings from an economic optimization approach, Energy. 189 (2019) 116194. https://doi.org/10.1016/j.energy.2019.116194.

[8] S. Quoilin, M.V.D. Broek, S. Declaye, P. Dewallef, V. Lemort, Techno-economic survey of Organic Rankine Cycle (ORC) systems, Renewable and Sustainable Energy Reviews. 22 (2013) 168–186. https://doi.org/10.1016/j.rser.2013.01.028.

[9] A. Atiz, M. Erden, M. Karakilcik, Energy and exergy analyses and electricity generation of PV-T combined with a solar collector for varying mass flow rate and ambient temperature, Heat Mass Transfer. 58 (2022) 1263–1278. https://doi.org/10.1007/s00231-022-03173-7.

[10] Y. Ding, E. Wang, G. Chen, The economic analysis of biomass gasification/direct combustion heating system, Journal of Hebei university of technology. 51 (2022) 65-72+92. https://doi.org/10.14081/j.cnki.hgdxb.2022.04.008.

[11] J. Wang, Research on Improved Low-temperature Solar Organic Rankine Cycle (ORC), Doctor, Tianjin University, 2009. https://kns.cnki.net/KCMS/detail/detail.aspx?dbcode=CMFD&dbname=CMFD2011&filename=2010091207.nh&v=.

[12] E. Wang, H. Zhang, B. Fan, Y. Wu, Optimized performances comparison of organic Rankine cycles for low grade waste heat recovery, J Mech Sci Technol. 26 (2012) 2301–2312. https://doi.org/10.1007/s12206-012-0603-4.

[13] N.B. Desai, S. Bandyopadhyay, Process integration of organic Rankine cycle, Energy. 34 (2009) 1674–1686. https://doi.org/10.1016/j.energy.2009.04.037.

[14] T. Yu, L. Liao, 冉 Liu, Thermal performance analysis of a combined reheating-regenerative-internal regenerative organic Rankine cycle, Thermal power generation. 45 (2016) 16–20. https://doi.org/10.3969/j.issn.1002-3364.2016.05.016.

[15] W. Zeng, Performance Analysis of Organic Rankine Cycle for Low Temperature Waste Heat Recovery on Ship, Doctor, Dalian Maritime University, 2019. https://kns.cnki.net/KCMS/detail/detail.aspx?dbcode=CMFD&dbname=CMFD202001&filename=1020016096.nh&v=.

[16] Z. Li, S. Khanmohammadi, S. Khanmohammadi, A.A.A.A. Al-Rashed, P. Ahmadi, M. Afrand, 3-E analysis and optimization of an organic rankine flash cycle integrated with a PEM fuel cell and geothermal energy, International Journal of Hydrogen Energy. 45 (2020) 2168–2185. https://doi.org/10.1016/j.ijhydene.2019.09.233.

[17] M. Mehrpooya, B. Ghorbani, A. Manizadeh, Cryogenic biogas upgrading process using solar energy (process integration, development, and energy analysis), Energy. 203 (2020) 117834. https://doi.org/10.1016/j.energy.2020.117834.

[18] D. Cocco, M. Petrollese, V. Tola, Exergy analysis of concentrating solar systems for heat and power production, Energy. 130 (2017) 192–203. https://doi.org/10.1016/j.energy.2017.04.112.

[19] M.G. Gado, S. Ookawara, S. Nada, H. Hassan, Renewable energy-based cascade adsorption-compression refrigeration system: Energy, exergy, exergoeconomic and enviroeconomic perspectives, Energy. 253 (2022) 124127. https://doi.org/10.1016/j.energy.2022.124127.

[20] L. Meyer, G. Tsatsaronis, J. Buchgeister, L. Schebek, Exergoenvironmental analysis for evaluation of the environmental impact of energy conversion systems, Energy. 34 (2009) 75–89. https://doi.org/10.1016/j.energy.2008.07.018.

[21] S. Wang, X. Liu, X. Gu, X. Huang, Y. Li, Analysis and multi-objective optimization of integrating a syngas-fed solid oxide fuel cell improved by a two-stage expander-organic flash cycle using an ejector and a desalination cycle, Energy. 272 (2023) 127095. https://doi.org/10.1016/j.energy.2023.127095.

[22] A. Shokri Kalan, S. Heidarabadi, M. Khaleghi, H. Ghiasirad, A. Skorek-Osikowska, Biomass-to-energy integrated trigeneration system using supercritical CO2 and modified Kalina cycles: Energy and exergy analysis, Energy. 270 (2023) 126845. https://doi.org/10.1016/j.energy.2023.126845.

[23] M.H. Khoshgoftar Manesh, M.J. Mehrabian, M. Nourpour, V.C. Onishi, Risk and 4E analyses and optimization of a novel solar-natural gas-driven polygeneration system based on

Integration of Gas Turbine–SCO2–ORC-solar PV-PEM electrolyzer, Energy. 263 (2023) 125777. https://doi.org/10.1016/j.energy.2022.125777.

[24] F. Cziesla, G. Tsatsaronis, Z. Gao, Avoidable thermodynamic inefficiencies and costs in an externally fired combined cycle power plant, Energy. 31 (2006) 1472–1489. https://doi.org/10.1016/j.energy.2005.08.001.

[25] S. Kelly, G. Tsatsaronis, T. Morosuk, Advanced exergetic analysis: Approaches for splitting the exergy destruction into endogenous and exogenous parts, Energy. 34 (2009) 384–391. https://doi.org/10.1016/j.energy.2008.12.007.

[26] A. Boyano, T. Morosuk, A.M. Blanco-Marigorta, G. Tsatsaronis, Conventional and advanced exergoenvironmental analysis of a steam methane reforming reactor for hydrogen production, Journal of Cleaner Production. 20 (2012) 152–160. https://doi.org/10.1016/j.jclepro.2011.07.027.

[27] A. Moharramian, S. Soltani, M.A. Rosen, S.M.S. Mahmoudi, M. Jafari, Conventional and enhanced thermodynamic and exergoeconomic analyses of a photovoltaic combined cycle with biomass post firing and hydrogen production, Applied Thermal Engineering. 160 (2019) 113996. https://doi.org/10.1016/j.applthermaleng.2019.113996.

[28] J. Oyekale, M. Petrollese, G. Cau, Modified auxiliary exergy costing in advanced exergoeconomic analysis applied to a hybrid solar-biomass organic Rankine cycle plant, Applied Energy. 268 (2020) 114888. https://doi.org/10.1016/j.apenergy.2020.114888.

[29] J. Oyekale, M. Petrollese, F. Heberle, D. Brüggemann, G. Cau, Exergetic and integrated exergoeconomic assessments of a hybrid solar-biomass organic Rankine cycle cogeneration plant, Energy Conversion and Management. 215 (2020) 112905. https://doi.org/10.1016/j.enconman.2020.112905.

[30] M.H. Khoshgoftar Manesh, E. Jadidi, Conventional and advanced exergy, exergoeconomic and exergoenvironmental analysis of a biomass integrated gasification combined cycle plant, Energy Sources, Part A: Recovery, Utilization, and Environmental Effects. (2020) 1–22. https://doi.org/10.1080/15567036.2020.1752856.

[31] A.K.S. Al-Sayyab, J. Navarro-Esbrí, V.M. Soto-Francés, A. Mota-Babiloni, Conventional and Advanced Exergoeconomic Analysis of a Compound Ejector-Heat Pump for Simultaneous Cooling and Heating, Energies. 14 (2021) 3511. https://doi.org/10.3390/en14123511.

[32] Y. Wang, G. Qin, Y. Zhang, S. Yang, C. Liu, C. Jia, Q. Cui, Conventional and advanced exergy analyses of an organic Rankine cycle by using the thermodynamic cycle approach, Energy Sci Eng. 9 (2021) 2474–2492. https://doi.org/10.1002/ese3.980.

[33] X. Hu, G. Li, S. Dong, P. Zhang, Advanced Exergy Analysis of Cascade High-temperature

Heat Pump System based on Experimental Data, Journal of engineering for thermal energy and power. 36 (2021) 87–93. https://doi.org/10.16146/j.cnki.rndlgc.2021.11.012.

[34] D.N. Özen, B. Koçak, Advanced exergy and exergo-economic analyses of a novel combined power system using the cold energy of liquefied natural gas, Energy. 248 (2022) 123531. https://doi.org/10.1016/j.energy.2022.123531.

[35] E.Y. Gürbüz, O.V. Güler, A. Keçebaş, Environmental impact assessment of a real geothermal driven power plant with two-stage ORC using enhanced exergo-environmental analysis, Renewable Energy. 185 (2022) 1110–1123. https://doi.org/10.1016/j.renene.2021.12.097.

[36] Z. Mohammadi, M. Fallah, Conventional and advanced exergy investigation of a double flash cycle integrated by absorption cooling, ORC, and TEG power system driven by geothermal energy, Energy. 282 (2023) 128372. https://doi.org/10.1016/j.energy.2023.128372.

[37] T. Li, X. Li, X. Gao, H. Gao, N. Meng, Geothermal power generation improvement of organic Rankine flash cycle using exergy, advanced exergy and exergoeconomic analyses, Applied Thermal Engineering. 223 (2023) 120032. https://doi.org/10.1016/j.applthermaleng.2023.120032.

[38] Z. Tian, X. Chen, Y. Zhang, W. Gao, W. Chen, H. Peng, Energy, conventional exergy and advanced exergy analysis of cryogenic recuperative organic rankine cycle, Energy. 268 (2023) 126648. https://doi.org/10.1016/j.energy.2023.126648.

[39] A. Moharramian, S. Soltani, M.A. Rosen, S.M.S. Mahmoudi, T. Bhattacharya, Modified exergy and modified exergoeconomic analyses of a solar based biomass co-fired cycle with hydrogen production, Energy. 167 (2019) 715–729. https://doi.org/10.1016/j.energy.2018.10.197.

[40] T. Hai, M.A. Ali, A. Alizadeh, S.F. Almojil, A.I. Almohana, A.F. Alali, Reduction in environmental CO2 by utilization of optimized energy scheme for power and fresh water generations based on different uses of biomass energy, Chemosphere. 319 (2023) 137847. https://doi.org/10.1016/j.chemosphere.2023.137847.

[41] A. Salari, A. Hakkaki-Fard, Thermodynamic analysis of a photovoltaic thermal system coupled with an organic Rankine cycle and a proton exchange membrane electrolysis cell, International Journal of Hydrogen Energy. 47 (2022) 17894–17913. https://doi.org/10.1016/j.ijhydene.2022.03.271.

[42] Y. Zhu, Thermodynamic Analysis and Economic Assessment of Biomass-fired Organic Rankine Cycle Combined Cooling Heat and Power System Integrated with Carbon Dioxide Capture, Doctor, Tianjin University, 2020.

https://kns.cnki.net/KCMS/detail/detail.aspx?dbcode=CDFD&dbname=CDFDLAST2022&filename=1021824776.nh&v=.

[43] Y. Zhu, W. Li, J. Li, H. Li, Y. Wang, S. Li, Thermodynamic analysis and economic assessment of biomass-fired organic Rankine cycle combined heat and power system integrated with CO2 capture, Energy Conversion and Management. 204 (2020) 112310. https://doi.org/10.1016/j.enconman.2019.112310.

[44] C. He, Z. Luo, G. Song, J. Yan, T. Pan, Research on the combustion emission of NO and CO from typical biomass soild fuel boilers in Tianjing, Environmental Engineering. 35 (2017) 86–90. https://doi.org/10.13205/j.hjgc.201704018.

[45] Y. Wang, J. Du, Q. Zhang, Y. Xin, W. Zhao, J. Chang, Research on Multiple Purification Device Design and Performance of Biomass Boiler Flue Gas, Transactions of the Chinese Society for Agricultural Machinery. 49 (2018) 313–318. https://doi.org/10.6041/j. issn.1000-1298.2018.02.040.

[46] T.T. Chow, Performance analysis of photovoltaic-thermal collector by explicit dynamic model, Solar Energy. 75 (2003) 143–152. https://doi.org/10.1016/j.solener.2003.07.001.

[47] A. James, M. Mohanraj, M. Srinivas, S. Jayaraj, Thermal analysis of heat pump systems using photovoltaic-thermal collectors: a review, J Therm Anal Calorim. 144 (2021) 1–39. https://doi.org/10.1007/s10973-020-09431-2.

[48] P. Ahmadi, I. Dincer, M.A. Rosen, Multi-objective optimization of a novel solar-based multigeneration energy system, Solar Energy. 108 (2014) 576–591. https://doi.org/10.1016/j.solener.2014.07.022.

[49] Y. Cao, H.A. Dhahad, A.G. ABo-Khalil, K. Sharma, A. Hussein Mohammed, A.E. Anqi, A.S. El-Shafay, Hydrogen production using solar energy and injection into a solid oxide fuel cell for CO2 emission reduction; Thermoeconomic assessment and tri-objective optimization, Sustainable Energy Technologies and Assessments. 50 (2022) 101767. https://doi.org/10.1016/j.seta.2021.101767.

[50] Z. Liu, T. Wei, D. Wu, Y. Zhang, G. Li, X. Yang, Performance Evaluation and Optimization of a Novel System Combining a Photovoltaic/Thermal Subsystem & an Organic Rankine Cycle Driven by Solar Parabolic Trough Collector, J. Therm. Sci. 30 (2021) 1513–1525. https://doi.org/10.1007/s11630-021-1503-7.

[51] X. Qi, O. Kochan, Z. Ma, P. Siarry, G. Królczyk, Z. Li, Energy, exergy, exergoeconomic and exergoenvironmental analyses of a hybrid renewable energy system with hydrogen fuel cells, International Journal of Hydrogen Energy. (2023) S0360319923036212. https://doi.org/10.1016/j.ijhydene.2023.07.163.

[52] R. Petela, Exergy of undiluted thermal radiation, Solar Energy. 74 (2003) 469–488. https://doi.org/10.1016/S0038-092X(03)00226-3.

[53] D. Chong, H. Zhou, X. Li, Y. Li, Exergoenvironmental analysis of a combined heat and power system for district heating using coal water slurry, Heating Ventilating & Air Conditioning. 52 (2022) 129–135. https://doi.org/10.19991/j.hvac1971.2022.07.20.

[54] L. Khani, S.M.S. Mahmoudi, A. Chitsaz, M.A. Rosen, Energy and exergoeconomic evaluation of a new power/cooling cogeneration system based on a solid oxide fuel cell, Energy. 94 (2016) 64–77. https://doi.org/10.1016/j.energy.2015.11.001.

[55] M. Teymouri, S. Sadeghi, M. Moghimi, S. Ghandehariun, 3E analysis and optimization of an innovative cogeneration system based on biomass gasification and solar photovoltaic thermal plant, Energy. 230 (2021) 120646. https://doi.org/10.1016/j.energy.2021.120646.

[56] M.A. Javadi, M. Khalili Abhari, R. Ghasemiasl, H. Ghomashi, Energy, exergy and exergy-economic analysis of a new multigeneration system based on double-flash geothermal power plant and solar power tower, Sustainable Energy Technologies and Assessments. 47 (2021) 101536. https://doi.org/10.1016/j.seta.2021.101536.

[57] Z.K. Mehrabadi, F.A. Boyaghchi, Exergoeconomic and exergoenvironmental analyses and optimization of a new low-CO2 emission energy system based on gasification-solid oxide fuel cell to produce power and freshwater using various fuels, Sustainable Production and Consumption. 26 (2021) 782–804. https://doi.org/10.1016/j.spc.2020.12.041.

[58] E.J.C. Cavalcanti, Exergoeconomic and exergoenvironmental analyses of an integrated solar combined cycle system, Renewable and Sustainable Energy Reviews. 67 (2017) 507–519. https://doi.org/10.1016/j.rser.2016.09.017.

[59] S.A. Mousavi Rabeti, M.H. Khoshgoftar Manesh, M. Amidpour, An innovative optimal 4E solar-biomass waste polygeneration system for power, methanol, and freshwater production, Journal of Cleaner Production. 412 (2023) 137267. https://doi.org/10.1016/j.jclepro.2023.137267.

[60] H. Vazini Modabber, S. Alireza Mousavi Rabeti, New optimal scheme for the poly-generation system, integrated with ORC and hydrogen production units, using technical, emergy, and thermo-risk analyses-case study for qeshm power and water co-generation plant, Thermal Science and Engineering Progress. 36 (2022) 101506. https://doi.org/10.1016/j.tsep.2022.101506.

[61] Y. Xu, S. Huang, J. Wang, M. Song, J. Yu, X. Shen, Energy and advanced exergy analyses of novel ejector-compressor partially coupled refrigeration cycle for buildings with less solar energy, Journal of Renewable and Sustainable Energy. 14 (2022) 043706.

https://doi.org/10.1063/5.0102885.

[62] E. Açıkkalp, A. Hepbasli, C.T. Yucer, T.H. Karakoc, Advanced exergoenvironmental assessment of a building from the primary energy transformation to the environment, Energy and Buildings. 89 (2015) 1–8. https://doi.org/10.1016/j.enbuild.2014.12.020.

[63] R. Najar, A. Kazemi, M. Borji, M. Nikian, Conventional and advanced exergy and exergoeconomic analysis of a biomass gasification based SOFC/GT cogeneration system, Journal of Renewable and Sustainable Energy. 15 (2023) 046303. https://doi.org/10.1063/5.0159977.